Association Study of Over 200,000 Subjects Detects Novel Rare Variants, Functional Elements, and Polygenic Architecture of Prostate Cancer Susceptibility

Nima C. Emami[1,2], Taylor B. Cavazos[1], Sara R. Rashkin[2], Clinton L. Cario[1,2], Rebecca E. Graff[2], Caroline G. Tai[2], Joel A. Mefford[3], Linda Kachuri[2], Eunice Wan[4], Simon Wong[4], David S. Aaronson[5], Joseph Presti[5], Laurel A. Habel[6], Jun Shan[6], Dilrini K. Ranatunga[6], Chun R. Chao[7], Nirupa R. Ghai[7], Eric Jorgenson[6], Lori C. Sakoda[6], Mark N. Kvale[4], Pui-Yan Kwok[3,4], Catherine Schaefer[6], Neil Risch[1-4,6,9], Thomas J. Hoffmann[1,2,4], Stephen K. Van Den Eeden[6,8], and John S. Witte[1-4,8,9]

[1]Program in Biological and Medical Informatics, University of California San Francisco, San Francisco, California, United States of America

[2]Department of Epidemiology and Biostatistics, University of California San Francisco, San Francisco, California, United States of America

[3]Program in Pharmaceutical Sciences and Pharmacogenomics, University of California San Francisco, San Francisco, California, United States of America

[4]Institute for Human Genetics, University of California San Francisco, San Francisco, California, United States of America

[5]Department of Urology, Kaiser Oakland Medical Center, Oakland, CA

[6]Division of Research, Kaiser Permanente Northern California, Oakland, CA

[7]Department of Research and Evaluation, Kaiser Permanente Southern California, Pasadena CA

[8]Department of Urology, University of California San Francisco, San Francisco, California, United States of America

[9]Helen Diller Family Comprehensive Cancer Center, University of California San Francisco, San Francisco, California, United States of America

ABSTRACT

The potential association between rare germline genetic variants and prostate cancer (PrCa) susceptibility has been understudied due to challenges with assessing rare variation. Furthermore, although common risk variants for PrCa have shown limited individual effect sizes, their cumulative effect may be of similar magnitude as high penetrance mutations. To identify rare variants associated with PrCa susceptibility, and better characterize the mechanisms and cumulative disease risk associated with common risk variants, we analyzed large population-based cohorts, custom genotyping microarrays, and imputation reference panels in an integrative study of PrCa genetic etiology. In particular, 11,649 men (6,196 PrCa cases, 5,453 controls) of European ancestry from the Kaiser Permanente Research Program on Genes, Environment and Health, ProHealth Study, and California Men's Health Study were genotyped and meta-analyzed with 196,269 European-ancestry male subjects (7,917 PrCa cases, 188,352 controls) from the UK Biobank. Six novel loci were genome-wide significant in our meta-analysis, including two rare variants (minor allele frequency < 0.01, at 3p21.31 and 8p12). Gene-based rare variant tests implicated a previously discovered PrCa gene (*HOXB13*) as well as a novel candidate (*ILDR1*) highly expressed in prostate tissue. Haplotypic patterns of long-range linkage disequilibrium were observed for rare genetic variants at *HOXB13* and other loci, reflecting their evolutionary history. Furthermore, a polygenic risk score (PRS) of 187 known, largely common PrCa variants was strongly associated with risk in non-Hispanic whites (90th vs. 10th decile OR = 7.66, $P = 1.80*10^{-239}$). Many of the 187 variants exhibited functional signatures of gene expression regulation or transcription factor binding, including a six-fold difference in log-probability of Androgen Receptor binding at the variant rs2680708 (17q22). Our finding of two novel rare variants associated with PrCa should motivate further consideration of the role of low frequency polymorphisms in PrCa, while the considerable effect of PrCa PRS profiles should prompt discussion of their role in clinical practice.

INTRODUCTION

For a number of diseases, including prostate cancer (PrCa), there has been limited success in detecting associated rare genetic variants, some of which may have substantial effect sizes [1]. This is in part due to the difficulty of measuring or imputing rare variants in adequately powered studies. Still, some rare germline variants associated with prostate cancer have been detected, such as in the DNA damage repair gene *BRCA2* [2] and the developmental transcription factor *HOXB13* [3]. While relatively few rare variants have been discovered, in aggregate they may comprise a substantial portion of PrCa risk heritability [4]. In contrast, genome-wide association studies (GWAS) of more common variants have identified over 150 independent genetic variants associated with PrCa [5]. Each variant is typically associated with only a modest increase in PrCa risk, and thus not of sufficient magnitude to be clinically significant. However, combining all associated variants together into a single polygenic risk score (PRS) may distinguish men with a meaningfully increased risk of PrCa.

To investigate the impact of rare and common variants on PrCa, we undertook a large scale genome-wide study of over 200,000 male subjects from two large cohorts: Kaiser Permanente (KP) in California [6] and the UK Biobank (UKB) [7]. Genotype microarrays, including GWAS backbones and custom rare variant content, were assayed in both cohorts, and unmeasured genotypes were imputed using a reference panel of over 27,000 phased Haplotype Reference Consortium (HRC) genomes [8]. We evaluated associations between individual rare and common variants and PrCa risk and interpreted the evolutionary origin and functional mechanisms of novel findings using multi-omics data. We also performed PRS modeling and functional characterization for the known common risk variants.

METHODS AND MATERIALS

Study Populations

We studied two cohorts of PrCa cases and non-diseased controls: 1) KP subjects from the Northern California Research Program on Genes, Environment and Health (RPGEH), the California Men's Health Study (CMHS) and the ProHealth Study; and 2) the UKB. The KP cohort included 6,196 male cases and 5,453 male controls of European-ancestry (mean age at diagnosis for cases = 68.1 years, mean age at baseline among controls = 71.5). The UKB cohort included 7,917 cases and 188,352 controls of European ancestry (mean age at diagnosis = 64.1, mean age among controls = 57.1). Subject demographics and characteristics are described in detail in Supplementary Table 1.

Custom Microarray Design and Genotyping

To directly assay or tag putatively functional rare variation in samples from KP, we collaborated with Affymetrix Inc. on the design of a custom Axiom DNA microarray (Supplementary Figure 1a) that was complementary to the GWAS array previously genotyped in the KP population [9]. The algorithm used to select variants on the custom array (Supplementary Figure 1b) resulted in 416,047 variant probesets comprising 54 distinct modules, including missense and loss-of-function mutations, rare exonic mutations from The Cancer Genome Atlas (TCGA) and dbGaP prostate cancer tumor exomes [10, 11], and variants to supplement the previously genotyped GWAS array [6] (Table 2). Many modules and most of the design content overlapped with the probesets on the UKB Affymetrix Axiom array, for which the array design, sample processing, and genotyping have been detailed [7].

Saliva biospecimens from KP participants were processed for DNA extraction using a protocol previously reported [9]. DNA samples from KP were processed using Samasy [12], a sample management system providing a visual and machine interface to facilitate robot liquid handling automation from source plates to destination plates matched by age, case status, and ethnicity. The algorithm implemented for destination plate randomization is described in the Supplementary Materials. A total of 173 96-well destination plates were amplified to increase DNA yields, and 200 ng of input DNA per well were array hybridized for 48 hours at 48 °C and genotyped using an Affymetrix GeneTitan Multi-Channel instrument.

Quality Control and Imputation

Detailed descriptions of the sample and genotype quality control (QC) procedures are given in the Supplementary Materials. Briefly, for the KP samples, we excluded specimens with poor resolution fluorescent measurements (DQC < 0.75) or call rate < 0.95 (Supplementary Figure 2a). Based on heterozygosity rate, call rate, and plate call rate, samples were further stratified into three tiers that were used to guide genotype quality control. Specifically, genotype calls and posterior cluster locations from higher tier samples (as a consequence of higher input DNA quantities) were prioritized and used as empirical priors for resolving genotypes of lower tier samples using the Affymetrix AxiomGT1 algorithm (Supplementary Figure 2b) [13]. Genotypes were also filtered based on batch differences across the RPGEH, CMHS, and ProHealth, and based on the fold-difference in minor allele frequency (MAF) relative to the HRC and 1000 Genomes Project reference panels. These genotypes were then merged with previously assayed GWAS genotypes for the KP subjects, whose QC was described in a prior publication [6].

The KP data were phased using Eagle v2.3 (cohort-based) [14], and imputed using Minimac3 to two reference panels: (1) a subpopulation of 27,165 HRC genomes accessible via the European Genome Archive (EGAS00001001710, which includes the 1000 Genomes Project Phase III samples), and (2) the 1000 Genomes Project Phase III reference panel (2,514 genomes). Single nucleotide variant calls were imputed using the union of (1) and (2), and indel polymorphisms were imputed using (2) (not yet part of the HRC due to additional difficulty in harmonizing indels; Supplementary Figure 3). Variants with $r^2_{INFO} < 0.3$ and with a minor allele frequency less than $1/N_{REF}$, where N_{REF} represents the total number of chromosomes in the reference panel, were removed from the imputed genotypes. Individuals were ultimately classified into ethnic analysis groups (African, East Asian, European, or Hispanic ancestry) based on self-reported ethnicity [15, 16], although only European ancestry subjects were retained for this study due to the sample size necessary to detect rare genetic variant associations.

For the UKB data, pre-imputation QC protocols have been previously described [7]. Genotypes were imputed using two reference panels: the complete HRC reference (64,976 haplotypes) [8], and the combined UK10K plus 1000 Genomes Project Phase III reference panels (9,746 haplotypes). We similarly excluded poorly imputed ($r^2_{\text{INFO}} < 0.3$) and excessively rare (MAF < $3*10^{-5}$) genotypes from the UKB.

Association Analyses

Associations between variant genotypes and prostate cancer were evaluated for European-ancestry subjects using logistic regression with adjustment for age (for PrCa cases, age at diagnosis, versus age at time of study enrollment for controls), body mass index, genotyping array, and principal components of ancestry (PCs). The KP models controlled for 20 PCs using PLINK v2.00 [17], and the UKB models were adjusted for 10 PCs. The KP and UKB data were combined by fixed-effect meta-analysis using Metasoft v2.0.0 [18]. Gene-based rare variant tests (observed MAF < 1%) were conducted with the Sequence Kernel Association Test (SKAT) using the rvtests package (v20171009) [19], and meta-analyzed by Fisher's method [20] using R v3.3.3.

Evolutionary History of Rare Variants

To quantify the recency in origin of rare prostate cancer risk variants, we examined the extended haplotype homozygosity (EHH), or the length of a haplotype on which a variant allele resides, using the reference panel of 27,165 phased HRC genomes and the selscan package [21]. We also quantified the integrative haplotype score (iHS), or log ratio between a variant's major and minor alleles of the area under the EHH curves for each allele [21], to reflect differences in allelic age or selective pressure between the derived and ancestral alleles. The iHS was computed using an EHH cutoff of 0.05, including both upstream (iHS_L) and downstream (iHS_R) of the query position.

Polygenic Risk Score Analyses

For each individual, their PRS was computed by multiplying the out-of-sample effect sizes [5,6] for each of the 187 previously reported PrCa risk loci (log ORs) by their genotype dosages, and then summing the resulting 187 values together (Supplementary Table 3). The odds ratios and 95% confidence intervals for associations between standardized PRS values (mean = 0, standard deviation = 1) and prostate cancer case-control status were estimated using logistic regression with adjustment for the same covariates modeled in our association analyses, with the exception of genotyping array so they could be compared.

Functional Annotation

To consider the functional relevance of the known PrCa risk variants, we integrated two different analyses and sources of data. We trained elastic net regression models of normal prostatic gene expression [22], with a linear combination of germline genotypes as the predictor, using GLMNet [23] and a dataset of 471 subjects with normal prostate tissue RNA expression and genotype data [24]. Among the 187 previously reported prostate cancer risk variants, as well as the novel genome-wide significant variants identified here, those directly modeled or in linkage disequilibrium (LD $r^2 > 0.5$) with a modeled variant in our expression models were reported. For the same set of variants, allele-specific differential transcription factor binding affinity was also estimated using sTRAP transcription factor affinity prediction [25] with the major and minor alleles.

RESULTS

Variant Association Analysis and Evolutionary Characterization

Genome-wide significant associations ($P_{\text{Meta}} < 5*10^{-8}$) were observed at six novel loci (>3 Mb away and LD $r^2 < 0.005$ in all 1000 Genomes Phase III populations, relative to known loci). Among the six loci (Figure 1; Table 1), three variants (rs557046152, rs555778703, and rs62262671) were at least nominally significant with consistent directions of effect in both the KP and UKB data, and two of these were rare imputed variants in European ancestry populations: rs557046152 (MAF = 0.003) and rs555778703 (MAF = 0.009). The remaining three variants were associated only in the UK Biobank. An additional gene-based rare variant meta-analysis of KP and UKB, using the sequence kernel association test (SKAT) and variants with MAF < 0.01, yielded a significant association at *HOXB13* ($P = 1.72*10^{-7}$; Supplementary Figure 4), a well-characterized prostate cancer risk locus harboring a rare yet highly penetrant missense founder mutation rs138213197 [3]. SKAT also identified a suggestive *P*-value for *ILDR1* ($P = 7.46*10^{-6}$), a gene primarily expressed in prostate tissue [26].

We observed atypically long-range LD for the previously identified rare *HOXB13* rs138213197, beyond a 1Mb window from the lead variant (Supplementary Figure 5). This observation was substantiated by considerable extended haplotype homozygosity for the rare missense allele (Figure 2a). In particular, rs138213197 had an integrated haplotype score (iHS) equal to 2.87 (iHS_L: 3.53, iHS_R: 2.54) in our HRC haplotype data, greater than the nominal |iHS| > 2 threshold, reflecting the recent origin or selective constraint at the rs138213197 locus. Likewise, for the novel rare variant rs555778703, the rare G risk allele (Figure 2b) had an iHS equal to 2.31 (iHS_L: 2.00, iHS_R: 2.79). For a proxy variant rs57029021 (LD r^2 = 0.666 in 1000 Genomes Project Phase III EUR) of the novel rare variant rs557046152 (which was unmeasured in the EGA HRC reference genomes), the rare A allele had an iHS equal to 0.87 (iHS_L: 1.60, iHS_R: 0.77; Figure 2c).

Polygenic Risk Scores and Functional Interpretation

For European-ancestry subjects in KP and UKB, there was a strong association between being in the top versus bottom decile of the PRS and prostate cancer (Supplementary Figure 6, Supplementary Table 4; OR [95% CI] = 7.66 [6.78, 8.64], $P = 1.80*10^{-239}$; OR_{KP_EUR} = 6.54 [5.45, 7.85], $P = 1.32*10^{-90}$; OR_{UKB_EUR} = 8.63 [7.18, 10.4], $P = 5.49*10^{-117}$).

To characterize the functional consequences of common variants, we examined their effects on gene expression and transcription factor binding. Among the 187 previously reported PrCa risk variants and 3 novel risk variants identified, 28 were in linkage disequilibrium (LD r^2 > 0.5 in 1000 Genomes Project Phase III EUR) with an expression quantitative trait locus (eQTL) variant in our regularized models of normal prostatic expression levels (Table 2). Furthermore, 21 variants were predicted to significantly alter transcription factor binding site (TFBS) affinities

(Table 3). rs2680708 (17q22) showed the greatest fold change in predicted binding affinity (log-difference P_{Binding} = 6.09) of any variant-TF pair analyzed (Table 3).

DISCUSSION

We combined imputed genotype data from two large cohorts totaling 14,113 PrCa cases and 201,722 controls, with a reference panel of over 27,000 phased genomes, to investigate the effects of rare genetic variants and the mechanisms and cumulative impact of common variants on PrCa risk. Three novel loci, including two rare variants (rs557046152 at 8p12, rs555778703 at 4q31.21) and one common variant (rs62262671 at 3p21.31), were associated with PrCa in our meta-analysis of European-ancestry subjects across cohorts. Likewise, an additional three novel variants were associated with PrCa in our meta-analysis, although this finding was driven primarily by the UKB participants.

Furthermore, the PRS associations we observed for European ancestry men were of larger magnitude of effect than reported previously, when there were only 105 known PrCa risk variants [6]. Namely, the nearly 8-fold increase in PrCa risk for men in the top vs. lowest decile of the PRS suggests that such a score may have similar predictive ability as high penetrance genes used to predict cancer risk in clinical practice, such as *BRCA1* (OR [95% CI]: 5.91 [5.25, 6.67]) and *BRCA2* (OR [95% CI]: 3.31 [2.95, 3.71]) for breast cancer risk [27]. Although the PRS effect is of relatively large magnitude, the scores may not be transferable to subjects of non-European descent [6], can be biased by genetic drift between ethnic groups [28], and could potentially widen existing health disparities [29].

Integration of gene expression and transcription factor binding site affinity data suggested novel mechanisms for many of the common PrCa variants previously reported. One example is a highly significant change in binding affinity at rs2680708. This finding is especially interesting given that rs2680708 abrogates a binding site for Androgen Receptor, a master regulator of prostatic gene expression. While our functional analyses did not nominate any genes whose expression may be affected as a consequence of eliminating this particular binding site, further study may reveal the effect of rs2680708 on the dysregulation gene expression or additional molecular processes. We also identified a putative mechanism of Oct1 binding for the newly implicated rs62262671 risk variant (3p21), which was predicted to have a large impact (log-difference P_{Binding} = 3.03) on binding affinity for Oct1, a TF with a known impact on PrCa and Androgen Receptor signaling [30]. Given that rs62262671 was also identified as an eQTL affecting the expression of *RBM6* and *UBA7*, these findings suggest that Oct1 may be involved in the regulation of the expression of these two genes, and provides a hypothesis for future functional follow-up regarding the involvement of these genes in prostate cancer development.

The mechanisms through which the rare, noncoding variants we identified are associated with prostate cancer remain somewhat unclear, with a lack of precise functional evidence regarding mechanism of action or close proximity to genes or known risk loci in *cis*. This underscores the challenge of not only detecting—but also interpreting—how rare variants impact the genetic etiology of complex traits using existing gene-based methodology and functional genomic datasets. Improved functional datasets may clarify the effects of rare variants on expression, splicing, or methylation.

Selective scans, which use population genetics metrics (such as EHH and iHS) to identify signatures of positive or negative natural selection [21], face similar challenges—rare variants naturally reside on longer haplotypes and obscure the direction of any selective forces that may act upon them [31]. If polymorphisms more exclusive, or even private, to a particular lineage or family comprise a substantial portion of disease risk for PrCa (or other traits), then new approaches and assays for both detecting and characterizing the relevant anomalies of these causal variants will be needed. These considerations are of particular importance given the proliferation of rare polymorphisms as a result of recent explosive human population expansion [32]. Hence, with the majority of all human variation shifting towards the low end of the allele frequency spectrum, identifying operative aberrations poses a significant challenge.

In spite of these challenges, over a decade of GWAS efforts [33] has advanced the genetic characterization of prostate cancer considerably. Our implementation of a PRS model for PrCa demonstrates this remarkable progress and the predictive power of aggregating PrCa risk loci.

CONCLUSIONS

By undertaking a GWAS in the large KP and UKB population-based cohorts, we detected multiple novel PrCa risk loci, including two rare variants, rs557046152 and rs555778703. Our PRS analysis of known common PrCa risk variants indicated that European ancestry men in the highest PRS decile have a substantially increased risk that may be of clinical importance; however, the result was greatly attenuated in other ancestries. Functional characterization of PrCa risk variants using gene expression and transcription factor binding affinity data revealed putative mechanisms. However, further study is needed to more fully illuminate the biological interactions that facilitate the influence of PrCa risk loci, in particular for rare variants.

AUTHOR CONTRIBUTIONS

John S. Witte had full access to all the data in the study and takes responsibility for the integrity of the data and the accuracy of the data analysis.

Study concept and design: Emami, Risch, Hoffmann, Van Den Eeden, Witte.

Acquisition of data: Cario, Mefford, Wan, Wong, Aaronson, Presti, Habel, Shan, Ranatunga, Chao, Ghai, Jorgenson, Sakoda, Kwok, Schaefer, Risch, Van Den Eeden, Witte.

Analysis and interpretation of data: Emami, Cavazos, Rashkin, Cario, Tai, Mefford, Kachuri, Kvale, Hoffmann, Witte.

Drafting of the manuscript: Emami, Graff, Witte.

Critical revision of the manuscript for important intellectual content: Emami, Hoffmann, Witte.

Statistical analysis: Emami, Cavazos, Rashkin, Witte.

Obtaining funding: Schaefer, Risch, Van Den Eeden, Witte.

Administrative, technical, or material support: None.

Supervision: Witte.

Other (specify): None.

Financial disclosures: John S. Witte certifies that all conflicts of interest, including specific financial interests and relationships and affiliations relevant to the subject matter or materials discussed in the manuscript (e.g. employment/affiliation, grants or funding, consultancies, honoraria, stock ownership or options, expert testimony, royalties, or patents filed, received, or pending), are the following: None.

Funding/Support and role of the sponsor: Supported by the Robert Wood Johnson Foundation, National Institutes of Health (R01CA088164, R01CA201358, R25CA112355, T32GM067547, and U01CA127298), the UCSF Goldberg-Benioff Program in Cancer Translational Biology, the UCSF Discovery Fellows program, the Microsoft Azure for Research program, and the Amazon AWS Cloud Credits for Research program. Support for participant enrollment, survey completion, and biospecimen collection for the RPGEH was provided by the Robert Wood Johnson Foundation, the Wayne and Gladys Valley Foundation, the Ellison Medical Foundation, and Kaiser Permanente national and regional community benefit programs. Genotyping of the GERA cohort was funded by a grant from the National Institute on Aging, the National Institute of Mental Health, and the NIH Common Fund (RC2 AG036607). The sponsors played no role in the study.

Acknowledgments: The authors thank Elad Ziv, Nadav Ahituv, and Ryan Hernandez for their guidance and feedback. Furthermore, we are grateful to the Kaiser Permanente Northern California members who have generously agreed to participate in the Kaiser Permanente Research Program on Genes, Environment, and Health, the ProHealth Study and the California Men's Health Study. This research has been conducted using the UK Biobank Resource under Application Number 14105.

APPENDIX A. Supplementary data

Supplementary data associated with this article can be found at the journal online.

REFERENCES

[1] Eichler EE, Flint J, Gibson G, Kong A, Leal SM, Moore JH, et al. Missing heritability and strategies for finding the underlying causes of complex disease. Nat Rev Genet. 2010;11:446-50.

[2] Ostrander EA, Udler MS. The role of the BRCA2 gene in susceptibility to prostate cancer revisited. Cancer Epidemiol Biomarkers Prev. 2008;17:1843-8.

[3] Ewing CM, Ray AM, Lange EM, Zuhlke KA, Robbins CM, Tembe WD, et al. Germline mutations in HOXB13 and prostate-cancer risk. N Engl J Med. 2012;366:141-9.

[4] Mancuso N, Rohland N, Rand KA, Tandon A, Allen A, Quinque D, et al. The contribution of rare variation to prostate cancer heritability. Nat Genet. 2016;48:30-5.

[5] Schumacher FR, Al Olama AA, Berndt SI, Benlloch S, Ahmed M, Saunders EJ, et al. Association analyses of more than 140,000 men identify 63 new prostate cancer susceptibility loci. Nat Genet. 2018;50:928-36.

[6] Hoffmann TJ, Van Den Eeden SK, Sakoda LC, Jorgenson E, Habel LA, Graff RE, et al. A large multiethnic genome-wide association study of prostate cancer identifies novel risk variants and substantial ethnic differences. Cancer Discov. 2015;5:878-91.

[7] Bycroft C, Freeman C, Petkova D, Band G, Elliott LT, Sharp K, et al. Genome-wide genetic data on ~500,000 UK Biobank participants. bioRxiv. 2017.

[8] McCarthy S, Das S, Kretzschmar W, Delaneau O, Wood AR, Teumer A, et al. A reference panel of 64,976 haplotypes for genotype imputation. Nat Genet. 2016;48:1279-83.

[9] Kvale MN, Hesselson S, Hoffmann TJ, Cao Y, Chan D, Connell S, et al. Genotyping Informatics and Quality Control for 100,000 Subjects in the Genetic Epidemiology Research on Adult Health and Aging (GERA) Cohort. Genetics. 2015;200:1051-60.

[10] Cancer Genome Atlas Research N. The Molecular Taxonomy of Primary Prostate Cancer. Cell. 2015;163:1011-25.

[11] Kumar A, White TA, MacKenzie AP, Clegg N, Lee C, Dumpit RF, et al. Exome sequencing identifies a spectrum of mutation frequencies in advanced and lethal prostate cancers. Proc Natl Acad Sci U S A. 2011;108:17087-92.

[12] Cario CL, Witte JS. Samasy: an automated system for sample selection and robotic transfer. Biotechniques. 2018;65:357-60.

[13] Thermo Fisher Scientific Inc. Axiom Genotyping Solution Data Analysis Guide. 2017.

[14] Loh PR, Danecek P, Palamara PF, Fuchsberger C, Y AR, H KF, et al. Reference-based phasing using the Haplotype Reference Consortium panel. Nat Genet. 2016;48:1443-8.

[15] Hoffmann TJ, Kvale MN, Hesselson SE, Zhan Y, Aquino C, Cao Y, et al. Next generation genome-wide association tool: design and coverage of a high-throughput European-optimized SNP array. Genomics. 2011;98:79-89.

[16] Hoffmann TJ, Zhan Y, Kvale MN, Hesselson SE, Gollub J, Iribarren C, et al. Design and coverage of high throughput genotyping arrays optimized for individuals of East Asian, African American, and Latino race/ethnicity using imputation and a novel hybrid SNP selection algorithm. Genomics. 2011;98:422-30.

[17] Chang CC, Chow CC, Tellier LC, Vattikuti S, Purcell SM, Lee JJ. Second-generation PLINK: rising to the challenge of larger and richer datasets. Gigascience. 2015;4:7.

[18] Han B, Eskin E. Random-effects model aimed at discovering associations in meta-analysis of genome-wide association studies. Am J Hum Genet. 2011;88:586-98.

[19] Zhan X, Hu Y, Li B, Abecasis GR, Liu DJ. RVTESTS: an efficient and comprehensive tool for rare variant association analysis using sequence data. Bioinformatics. 2016;32:1423-6.

[20] Lee S, Teslovich TM, Boehnke M, Lin X. General framework for meta-analysis of rare variants in sequencing association studies. Am J Hum Genet. 2013;93:42-53.

[21] Szpiech ZA, Hernandez RD. selscan: an efficient multithreaded program to perform EHH-based scans for positive selection. Mol Biol Evol. 2014;31:2824-7.

[22] Emami NC, Kachuri L, Meyers TJ, Das R, Hoffman JD, Hoffmann TJ, et al. Association of imputed prostate cancer transcriptome with disease risk reveals novel mechanisms. Nat Commun. 2019;10:3107.

[23] Friedman J, Hastie T, Tibshirani R. Regularization Paths for Generalized Linear Models via Coordinate Descent. J Stat Softw. 2010;33:1-22.

[24] Thibodeau SN, French AJ, McDonnell SK, Cheville J, Middha S, Tillmans L, et al. Identification of candidate genes for prostate cancer-risk SNPs utilizing a normal prostate tissue eQTL data set. Nat Commun. 2015;6:8653.

[25] Manke T, Roider HG, Vingron M. Statistical modeling of transcription factor binding affinities predicts regulatory interactions. PLoS Comput Biol. 2008;4:e1000039.

[26] Hauge H, Patzke S, Delabie J, Aasheim HC. Characterization of a novel immunoglobulin-like domain containing receptor. Biochem Biophys Res Commun. 2004;323:970-8.

[27] Kurian AW, Hughes E, Handorf EA, Gutin A, Allen B, Hartman A-R, et al. Breast and ovarian cancer penetrance estimates derived from germline multiple-gene sequencing results in women. J Clin Oncol Precision Oncol. 2017;(1):1-12.

[28] Martin AR, Gignoux CR, Walters RK, Wojcik GL, Neale BM, Gravel S, et al. Human Demographic History Impacts Genetic Risk Prediction across Diverse Populations. Am J Hum Genet. 2017;100:635-49.

[29] Martin AR, Kanai M, Kamatani Y, Okada Y, Neale BM, Daly MJ. Current clinical use of polygenic scores will risk exacerbating health disparities. Nat Genet. 2019;51:584-91.

[30] Obinata D, Takayama K, Fujiwara K, Suzuki T, Tsutsumi S, Fukuda N, et al. Targeting Oct1 genomic function inhibits androgen receptor signaling and castration-resistant prostate cancer growth. Oncogene. 2016;35:6350-8.

[31] Maruyama T. The age of an allele in a finite population. Genet Res. 1974;23:137-43.

[32] Uricchio LH, Zaitlen NA, Ye CJ, Witte JS, Hernandez RD. Selection and explosive growth alter genetic architecture and hamper the detection of causal rare variants. Genome Res. 2016;26:863-73.

[33] Visscher PM, Wray NR, Zhang Q, Sklar P, McCarthy MI, Brown MA, et al. 10 Years of GWAS Discovery: Biology, Function, and Translation. Am J Hum Genet. 2017;101:5-22.

TABLES

Table 1. Novel Prostate Cancer Susceptibility Associations from the Meta-Analysis of European Ancestry Subjects from Kaiser Permanente and UK Biobank

Risk Variant **dbSNP rsid** *Genomic Locus* *gnomAD MAF* *Risk Allele (Ref)*	**Kaiser Permanente (KP)** **EUR Subjects** **(6,196 cases, 5,453 controls)**			**UK Biobank (UKB)** **EUR Subjects** **(7,917 cases, 188,352 controls)**			**Meta-Analysis** **KP + UKB EUR Subjects**	
	Odds Ratio [95% CI]	***P*-value**	r^2_{INFO}	**Odds Ratio [95% CI]**	***P*-value**	r^2_{INFO}	**Odds Ratio [95% CI]**	***P*-value**
rs557046152 *Locus*: 8p12 *MAF*: 0.003* G (GTT)	2.26 [1.72, 2.96]	$3.70*10^{-9}$	0.94	1.40 [1.06, 1.85]	0.019	0.85	1.79 [1.47, 2.17]	$4.50*10^{-9}$
rs555778703 *Locus*: 4q31.21 *MAF*: 0.009 G (A)	1.54 [1.08, 2.17]	0.016	0.50	2.00 [1.54, 2.58]	$1.64*10^{-7}$	0.74	1.82 [1.48, 2.24]	$1.65*10^{-8}$
rs62262671 *Locus: 3p21.31* *MAF: 0.133* G (A)	1.18 [1.09, 1.27]	$3.47*10^{-5}$	0.98	1.10 [1.05, 1.15]	$7.56*10^{-5}$	1.0	1.12 [1.07, 1.16]	$3.55*10^{-8}$
Significantly Associated Variants in Meta-Analysis, Absent Nominal Significance in Both Cohorts								
rs80242938 *Locus*: 16p13.3 *MAF*: 0.0002 G (A)	7.10 [$9.5*10^{-5}$, $5.3*10^{6}$]	0.73	0.67	11.7 [5.17, 26.7]	$4.18*10^{-9}$	0.80	11.7 [5.16, 26.6]	$3.95*10^{-9}$
rs149892036 *Locus*: 8q12.1 *MAF*: 0.001 T (C)	1.53 [0.81, 2.88]	0.19	0.80	2.31 [1.71, 3.12]	$5.37*10^{-8}$	0.85	2.14 [1.63, 2.81]	$4.32*10^{-8}$
rs139191981 *Locus*: 3q26.33 *MAF*: 0.0005 A (G)	0.88 [0.19, 4.09]	0.88	0.90	7.62 [3.93, 14.8]	$1.87*10^{-9}$	0.92	5.43 [2.95, 9.97]	$4.96*10^{-8}$

* rs557046152 (merged into rs78795568 in dbSNP build 151) minor allele frequency from 1000 Genomes Project Phase III EUR (not present in gnomAD). Remaining minor allele frequencies from gnomAD European (non-Finnish) frequency.

Table 2. Normal Prostate Tissue Expression eQTLs Correlated with PrCa Risk Variants

Previously Reported PrCa Risk Variant	**Gene Name**	**Number of eQTL Variants Targeting Gene and with LD r^2 > 0.5 with Risk Variant**	**eQTL Variants (chr.hg19pos.ref.alt)**
rs17599629	LYSMD1	1 eQTLs	rs17599629 (chr1.150658287.A.G)
rs1775148	RAB7L1	1 eQTLs	rs1775148 (chr1.205757824.C.T)
rs13385191	C2orf43	1 eQTLs	rs13385191 (chr2.20888265.A.G)
rs2430386	EHBP1	3 eQTLs	rs201697978 (chr2.62876580.A.C), rs12713462 (chr2.62804482.C.T), rs142973842 (chr2.63056706.TTG.T)
rs13016083	ACVR2A	4 eQTLs	rs7423878 (chr2.148689369.T.C), rs7600869 (chr2.148551232.C.G), rs70992173 (chr2.148570502.AT.A), rs1424949 (chr2.148542963.T.G)
rs62262671	RBM6	1 eQTLs	rs62262671 (chr3.49649873.A.G)
	UBA7	1 eQTLs	rs62262671 (chr3.49649873.A.G)
rs12653946	IRX4	1 eQTLs	rs12653946 (chr5.1895829.C.T)
rs1983891	FOXP4	5 eQTLs	rs913074 (chr6.41538545.T.C), rs4714486 (chr6.41542417.C.T), rs4714485 (chr6.41536587.T.G), rs1886816 (chr6.41544494.A.G), rs6458228 (chr6.41543793.C.A)
rs9469899	UHRF1BP1	1 eQTLs	rs9469899 (chr6.34793124.G.A)
rs1933488	RGS17	1 eQTLs	rs6557267 (chr6.153433701.C.T)
rs9364554	SLC22A3	2 eQTLs	rs1112444 (chr6.160835192.C.A), rs9364554 (chr6.160833664.C.T)
rs6465657	BHLHA15	1 eQTLs	rs6465657 (chr7.97816327.C.T)
rs1182	C9orf78	5 eQTLs	rs55946414 (chr9.132583289.A.T), rs1043186 (chr9.132573290.C.T), rs3842225 (chr9.132575426.GC.G), rs11787741 (chr9.132578284.A.G), rs13283469 (chr9.132582014.C.T)
rs10993994	MSMB	1 eQTLs	rs10993994 (chr10.51549496.T.C)
	NCOA4	1 eQTLs	rs10993994 (chr10.51549496.T.C)
	AGAP7	1 eQTLs	rs10993994 (chr10.51549496.T.C)
rs4962416	CTBP2	5 eQTLs	rs4962416 (chr10.126696872.T.C), rs12769019 (chr10.126697327.A.G), rs4962720 (chr10.126696840.G.T), rs12769682 (chr10.126697494.G.C), rs4962419 (chr10.126697114.G.A)
rs61890184	PPFIBP2	1 eQTLs	rs61890184 (chr11.7547587.G.A)
rs12785905	SYT12	2 eQTLs	rs12785905 (chr11.66951965.G.C), rs12785906 (chr11.66951966.G.C)

Previously Reported PrCa Risk Variant	**Gene Name**	**Number of eQTL Variants Targeting Gene and with LD r^2 > 0.5 with Risk Variant**	**eQTL Variants (chr.hg19pos.ref.alt)**
rs11568818	MMP7	1 eQTLs	rs11568818 (chr11.102401661.T.C)
rs11214775	TMPRSS5	1 eQTLs	rs11214775 (chr11.113807181.G.A)
rs138466039	PKNOX2	1 eQTLs	rs138466039 (chr11.125054793.C.T)
rs80130819	COL2A1	1 eQTLs	rs80130819 (chr12.48419618.A.C)
rs684232	FAM57A	2 eQTLs	rs2474694 (chr17.618039.G.A), rs684232 (chr17.618965.T.C)
	GEMIN4	2 eQTLs	rs2474694 (chr17.618039.G.A), rs684232 (chr17.618965.T.C)
rs142444269	C17orf79	1 eQTLs	rs142444269 (chr17.30098749.C.T)
rs12956892	SEC11C	16 eQTLs	rs4940816 (chr18.56745159.A.G), rs4940817 (chr18.56745263.T.G), rs4940815 (chr18.56745144.A.G), rs4940812 (chr18.56742965.G.A), rs4940810 (chr18.56742446.T.C), rs4940811 (chr18.56742904.A.G), rs12956892 (chr18.56746315.G.T), rs12327532 (chr18.56744666.T.G), rs12326997 (chr18.56743138.A.G), rs12327517 (chr18.56744475.T.C), rs12327515 (chr18.56744457.T.C), s10579935 (chr18.56742710.GTAAA.G), rs12327308 (chr18.56743208.T.G), rs4940809 (chr18.56742291.T.C), rs34192989 (chr18.56744092.T.C), rs4940442 (chr18.56742873.A.G)
rs7241993	ATP9B	1 eQTLs	rs9967549 (chr18.76774276.A.C)
rs8102476	CATSPERG	2 eQTLs	rs8102476 (chr19.38735613.C.T), rs8102454 (chr19.38735480.G.A)
	PPP1R14A	2 eQTLs	rs8102476 (chr19.38735613.C.T), rs8102454 (chr19.38735480.G.A)
rs5945572	NUDT11	5 eQTLs	rs1327304 (chrX.51214176.C.A), rs1327302 (chrX.51210615.G.A), rs5945572 (chrX.51229683.A.G), rs58498379 (chrX.51223415.C.T), rs1327303 (chrX.51214169.C.T)
rs4844289	NLGN3	1 eQTLs	rs4844289 (chrX.70407983.A.G)

Table 3. Predicted Impact of PrCa Risk Variants on Transcription Factor Binding Affinity

Previously Reported PrCa Risk Variant *Genomic Locus* *Risk Allele (Alt)*	**Transcription Factor**	**$P_{Binding}$ Risk Allele**	**$P_{Binding}$ Alt Allele**	**Log-Difference in Transcription Factor Binding *P*-value Between Risk Allele and Alternate Allele**	**TRANSFAC Vertebrate 2010.1 Matrix Name**
rs2680708 *17q22* *G (A)*	AR	0.49	3.91E-07	6.09	AR_Q6
	DBP	0.13	3.91E-07	5.53	DBP_Q6
rs5799921 *12q21.33* *GA (G)*	HMGIY	0.37	3.38E-07	6.04	HMGIY_Q6
rs2660753 *3p12.1* *T (C)*	AP1	0.55	2.10E-06	5.42	AP1_Q6_01
		0.42	2.10E-06	5.3	AP1_Q4_01
rs7210100 *17q21.33* *A (G)*	DELTAEF1	0.57	2.31E-06	5.39	DELTAEF1_01
rs9600079 *13q22.1* *T (G)*	TATA	8.98E-07	0.15	5.22	TATA_C
rs742134 *22q13.2* *G (A)*	STAT5A	0.01	4.03E-08	5.12	STAT5A_03
	HNF1	2.70E-03	4.03E-08	4.83	HNF1_Q6_01
rs9625483 *22q12.1* *A (G)*	MAFB	1.56E-06	0.2	5.1	MAFB_01
rs5759167 *22q13.2* *G (T)*	DBP	0.07	9.55E-07	4.84	DBP_Q6
rs10086908 *8q24.21* *T (C)*	GATA3	2.39E-06	0.07	4.47	GATA3_01
rs59308963 *2q33.1* *- (ATTCTGTC)*	TCF11	1.44E-05	0.37	4.41	TCF11_01
rs1935581 *10q23.31* *C (T)*	STAT1	3.43E-06	0.06	4.27	STAT1_03
	STAT4	3.43E-06	0.05	4.16	STAT4_01
rs4245739 *1q32.1* *A (C)*	HNF4	6.83E-05	0.98	4.16	HNF4_Q6_02
rs1283104 *3q13.12* *G (C)*	FXR	7.42E-04	5.35E-08	4.14	FXR_Q2

Previously Reported PrCa Risk Variant *Genomic Locus* *Risk Allele (Alt)*	**Transcription Factor**	P_{Binding} **Risk Allele**	P_{Binding} **Alt Allele**	**Log-Difference in Transcription Factor Binding *P*-value Between Risk Allele and Alternate Allele**	**TRANSFAC Vertebrate 2010.1 Matrix Name**
rs76551843 *5q35.1* *A (G)*	IPF1	4.73E-05	0.58	4.09	IPF1_Q6
rs6869841 *5q35.2* *A (G)*	HOXA3	0.29	4.25E-05	3.84	HOXA3_01
rs13385191 *2p24.1* *G (A)*	NFAT1	0.39	5.95E-05	3.82	NFAT1_Q6
rs1571801 *9q33.2* *A (C)*	ZNF333	4.16E-05	0.27	3.82	ZNF333_01
rs339331 *6q22.1* *T (C)*	IRF8	0.37	6.58E-05	3.75	IRF8_Q6
rs1283104 *3q13.12* *G (C)*	PNR	2.66E-04	5.35E-08	3.7	PNR_01
rs182314334 *3q25.1* *T (C)*	POU1F1	0.04	7.81E-06	3.69	POU1F1_Q6
rs17694493 *9p21.3* *G (C)*	STAT	0.34	8.04E-05	3.62	STAT_Q6

FIGURES

Figure 1. Prostate Cancer Risk Meta-Analysis Manhattan Plot for Kaiser Permanente and UK Biobank European-Ancestry Subjects

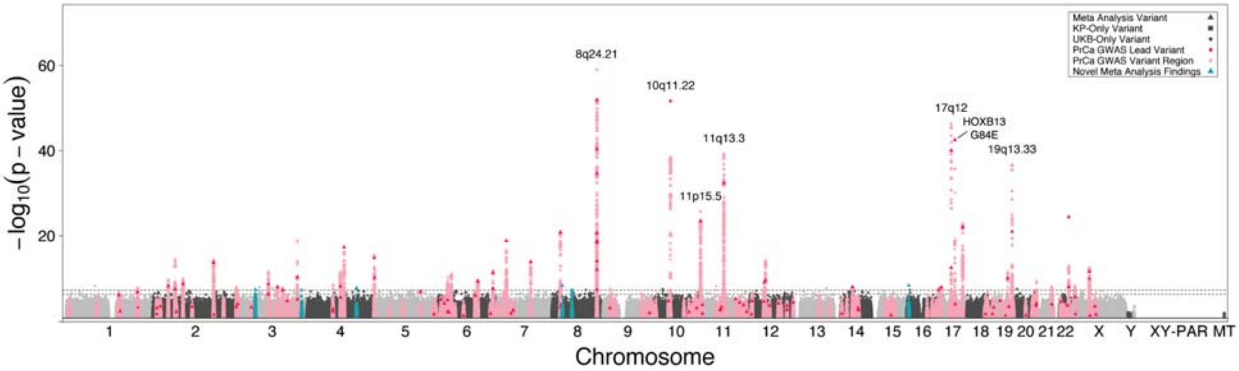

Figure 1 Legend: Genome-Wide Manhattan Plot of Prostate Cancer Risk. Manhattan plot depicting the results of a meta-analysis of male European-ancestry subjects from the Kaiser Permanente (KP; N = 6,196 PrCa cases, 5,453 controls) and UK Biobank (UKB; N = 7,917 PrCa cases, 188,352 controls) cohort genome-wide associations with prostate cancer (PrCa) risk. The associations (-$\log_{10}$(*P*-value), Y-axis) are plotted against the chromosome (1-22, X, Y, XY-pseudoautosomal region XY-PAR, and mitochondrial chromosome MT) and position (X-axis) of the genotyped or imputed genetic variants, with thresholds for significant ($P < 5.0*10^{-8}$) and suggestive ($5.0*10^{-7} < P < 5.0*10^{-8}$) associations illustrated by dashed grey lines. Non-significant loci on odd and even chromosomes are colored in alternating shades, and all variants with $P > 0.05$ are excluded from the plot. Triangular data points illustrate variants that were meta-analyzed between KP and UKB, while squares and circles indicate variants present exclusively in the KP or UKB summary statistics, respectively. Previously discovered PrCa loci are highlighted in pink for a 2 Mb window around the reported lead variant, which is highlighted in red, and previously unreported loci reaching genome-wide significance in our meta-analysis are colored in teal.

Figure 2. Extended Haplotype Homozygosity of Prostate Cancer Associated Rare Variants

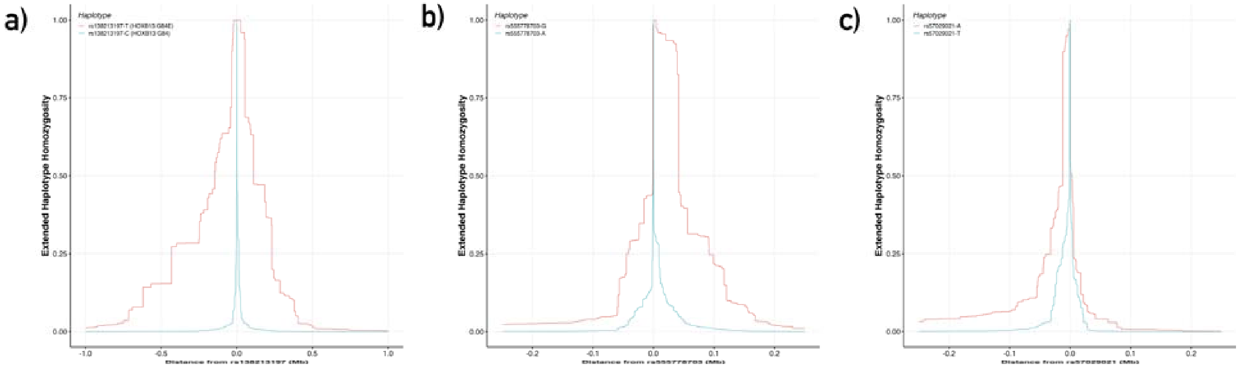

Figure 2 Legend: "Haplotype Lengths for Rare PrCa Risk Variants. Extended haplotype homozygosity (EHH) plots illustrating the decay in non-recombinant linkage (Y-axis) with increasing distance along the length of the haplotypes centered at two alleles of a "core" query variant (X-axis). Differences in EHH, iHH (the area under the EHH curve), and iHS (the log-ratio between the iHH for the derived and ancestral allele) may reflect a difference in allelic age between the derived and ancestral alleles, or alternatively the selective pressure to retain a particular allele with preference to the alternative. 2a. EHH curves for the rare *HOXB13* G84E missense variant and Northern European founder mutation rs138213197, for which the iHS value of 2.87 (iHS_L: 3.53, iHS_R: 2.54) reflects the more recent origin of the derived G84E allele rs138213197-T. 2b. EHH curves for the novel rare variant association rs555778703, with an iHS value of 2.31 (iHS_L: 2.00, iHS_R: 2.79). 2c. EHH curves for rs57029021, an LD proxy variant for the novel rare indel association rs557046152 (LD r^2 = 0.666 in 1000 Genomes Project Phase III EUR) with an iHS value of 0.87 (iHS_L: 1.60, iHS_R: 0.77)."

SUPPLEMENTARY MATERIALS

Custom Microarray Design and Genotyping

In our design of a DNA microarray with predominantly custom, functionally relevant markers, the SNP selection procedure was conducted as follows. First, a set of target markers was constructed. This target set included variants previously associated in genome-wide association studies (GWAS), significant and suggestive, of prostate cancer (PrCa) associated traits (PSA level, gene-by-gene interactions), other correlated traits (breast cancer, height, body mass index, obesity, diabetes, and others), and also uncorrelated traits (all NHGRI GWAS catalog traits). Additionally, a set of pan-cancer candidate genes was compiled by experimental colleagues, and all rare variants in windows centered around these genes were included in the target set. Rare variant in windows around highly mutated genes from the somatic cancer database COSMIC were also included. Furthermore, rare variants from a series of whole genome and whole exome sequence analyses (of African American PrCa case normal genomes [1], The Cancer Genome Atlas (TCGA) [2] and dbGaP [3] normal exomes, and ENCODE PrCa DNAse I hypersensitive regions) were put into the target set.

Second, variant selection was conducted with complementarity to the GWAS array previously assayed in the study population in order to limit redundancy (Supplementary Figure 1b), drawing from a candidate set disjoint from the GWAS array markers. This produced a set of primarily rare selected markers optimized for coverage of the target set, through tagging and direct genotyping (Supplementary Figure 1a; Supplementary Table 2).

Genotyping sample DNA plates without special attention to matching case and control covariates can lead to batch effects. In order to minimize batch effects and expedite genotyping, a sample management system (Samasy) [4] and sample selection algorithm were designed and implemented to robot-automate DNA sample allocation. The greedy sample selection algorithm for moving case and control DNA samples from source plates to destination plates was designed with the following objectives: 1) Use all available PrCa cases on source plates, 2) Select equal numbers of controls and cases, 3) Frequency match the distribution of race and age in controls and cases, while oversampling African American controls and rare (race and age) strata to improve power, 4) Select all required samples from a source plate at one time so lab workers will only have to locate and handle a source plate once, 5) Optimize work flow so sets of source and destination plates can be simultaneously loaded and unloaded from the Biomek liquid handling robot.

Quality Control and Imputation

The quality control (QC) process is described in Supplementary Figures 2a and 2b.

In order to produce the highest confidence genotype calls for the greatest number of samples and probesets, sample quality was first evaluated to screen for and eliminate potential outliers that may negatively impact downstream genotype clustering. Sample QC was executed in three stages. First, signal-to-noise (DishQC (DQC), ranging from 0 to 1) was computed for each sample based on intensity data calculated from the raw microarray fluorescence images. A threshold was drawn to exclude samples with low signal-to-noise (DQC < 0.75) based on the inflection point of the empirical distribution of DQC values. Second, 20,000 diagnostic Step 1 probesets were genotyped using 5 sample batches (grouped chronologically based on sample processing dates) to obtain empirical distributions of sample call rates for each batch. A call rate threshold was drawn based on the inflection points of these distributions to exclude samples with low call rates (CR < 0.95) or missing covariates from further analyses, leaving 14,818 samples. Third, the remaining samples were re-genotyped at all 416,047 Step 2 probesets using the same chronological packaging. Correlations between heterozygosity rate and call rate were used to define three clustered tiers (Supplementary Figure 2a) of sample quality: higher quality samples (HQ, with Call Rate > 97% and Heterozygosity Rate < 15%), lower quality samples (LQ), and plate quality control (PQC) samples (Plate Call Rate < 96.5%). Finally, among 80 pairs of samples with a high, 1st degree level of relatedness (kinship coefficient > 0.35), one of each pair of individuals was removed from further analysis, preferentially retaining prostate cancer cases. This concluded sample QC and provided a basis for evaluating QC of probesets through additional re-genotyping.

Given the remaining 14,818 samples, each labeled according to three tiers of sample quality outlined above, re-genotyping was performed to separate well resolved probesets from those susceptible to batch effects, and strategies were implemented to correct for these batch effects for the greatest number of probesets. First, all 14,818 samples, regardless of tier, were genotyped across all 416,047 probesets. Genotype clusters were next evaluated across all probesets, and classified as being either well resolved across all samples (i.e. not susceptible to batch effects, n=327,703), well resolved across only HQ samples (n=6,672), or poorly resolved (n=81,672). In order to remedy batch effects, first the probesets resolved in the HQ samples were considered. An Empirical Bayes genotyping strategy was implemented in which the well resolved HQ genotype clusters were used to sequentially guide the genotyping of samples in the lower quality LQ and PQC tiers. By packaging LQ tiers with HQ tiers, and using the posterior HQ cluster centers as AxiomGT1 [5] priors for re-genotyping, genotype calls were produced for each probeset across all sample tiers. Minor allele frequency (MAF) was compared among sample tiers in order to identify probesets where call frequencies were in agreement and in disagreement. Genotype calls for which MAF agreed among tiers (within 10% of HQ samples MAF) were retained as final genotypes for their respective probesets, while those probesets exhibiting MAF disagreements among tiers were combined with the other poorly resolved probesets for a series of procedures.

These procedures included re-thresholding the genotype cluster metric Heterozygous Strength Offset, which measures the displacement of the heterozygous cluster in relation to the homozygous clusters, as well as using linear regression to normalize probeset intensities across plates. The latter procedure led to the reclassification of 15,319 probesets as well resolved, and 65,177 as poorly resolved. These poorly resolved variants were processed through additional steps (Supplementary Figure 2b) to identify monomorphic probesets based on a genotype cluster metric Homozygote Ratio Offset (HomRO) and isolate calls for only HQ samples. The probesets well resolved in only HQ samples, in addition to those reclassified by plate-normalization, were combined with the remaining well-resolved probesets for optimization of both polymorphic probeset detection sensitivity (Minor Homozygote, Het Cluster Strengthening) and also rare variant detection sensitivity (Rare Variant Per-Plate Re-Genotyping).

After the conclusion of the preceding raw genotype QC steps described above and outlined in Supplementary Figure 2b, several additional QC steps were performed on the called genotypes for the genotype-resolved variants (n=356,671). First, variants that deviated from Hardy-Weinberg Equilibrium (p < 1e-4) in European ancestry controls were removed (n=30,632), leaving n=326,039 variants. Next, to further control for batch effects, variants where genotype was associated with sample quality tier (HQ vs. LQ; p < 1e-4) were further excluded (n=1,376). Furthermore, variants where European ancestry minor allele frequency deviated from the Thousand Genomes Project EUR MAF [6] by greater than 10% (n=164) or that were monomorphic (n=69,431) were filtered out, leaving n=255,068 variants remaining. Furthermore, variants with low AxiomGT1 genotype clustering confidence scores (less than 0.2) were identified (n=22,560) and excluded from further analysis. Finally, variants which evaded prior QC but whose cluster plots upon visual inspection raised suspicion of a cluster split (i.e. misclustering by the AxiomGT1 algorithm, leading to misclassification of homozygotes as heterozygotes, or vice versa) were excluded (n=100), yielding a final total of 232,408 variants for phasing, imputation, and downstream analysis.

Evolutionary History of Rare Variants

For generating a genetic map to be used in calculating EHH and iHS, the predictGMAP program [7] was used to interpolate genetic map positions, using 1000 Genomes Project OMNI genetic map files as a reference [8]. The selscan package [9] was run with the settings “--keep-low-freq”, “--max-extend 0”, “--threads 8”, and “--ehh-win 500000,” with the exception that “--ehh-win 1000000” was invoked for the *HOXB13* G84E mutation rs138213197 to account for longer range LD. The integrative haplotype score (iHS) was computed manually using a python script implementing equations (4) and (5) from the selscan publication [9].

Polygenic Risk Score Analyses

Polygenic risk scores (PRS) of PrCa risk were computed by taking sum of the effect sizes for 187 previously reported PrCa risk loci [10-31] (Table 3). This included the 105 variants previously modeled by Hoffmann et al. in 2015 [32], the 63 novel variants discovered by Schumacher et al. in 2018 in the European-ancestry PRACTICAL consortium [33], as well as summary statistics reported for an additional 20 independent variants (LD $r^2 \leq 0.3$ in 1000 Genomes Project Phase III EUR) [34-38].

Functional Annotation

To interpret the functional relevance of the known PrCa risk variants, we trained elastic net regression models of normal prostatic gene expression [39]. Training samples with paired genotype and gene expression data were drawn from the National Center for Biotechnology Information (NCBI) publicly available database of Genotypes and Phenotypes (dbGaP phs000985.v1.p1). Training data derived from a study which collected histologically normal prostate tissue from consenting subjects (471 European-ancestry men; mean age [SD]: 60.1 [7.15] for the 249 men with age available) having undergone radical prostatectomy treatment for prostate cancer (N = 453; 63.6% Gleason 6, 36.4% Gleason 7) or cystoprostatectomy treatment for bladder cancer (N = 18). Inclusion criteria, histopathological assessment, sample processing, and quality control were described previously for these data [40].

We imputed unobserved training data genotypes to the 1000 Genomes Project Phase III reference panel using a pre-phasing workflow to match the strand and reference allele recorded in the data with those observed in the reference panel, while excluding ambiguous variants and indel mutations. Next, samples were phased and imputed using Eagle v2.3 [41] (cohort-based) and Beagle v4.1 [42], respectively. Gene boundaries (hg38) for 17,233 transcripts were downloaded from the NCBI Gene database using the Biopython Entrez eutils REST API [43]. Genomic coordinates were converted from hg38 to hg19 (GRCh37) via UCSC liftOver. For each transcript, well-imputed ($r^2_{INFO} > 0.8$) training data genetic variants located (a) in the within 500kb of the start position, (b) between the start and end positions, inclusive, or (c) within 500kb of the end position, were extracted. Next, following the PrediXcan gene expression model training procedure [44], a regularized regression model was fit with the R (v3.2.2) package GLMNet [45], with genetic variants *in cis* to a given transcript as the design matrix, and the transcript RNA-Seq RPKM levels as the response variable. Models with at minimum one non-intercept explanatory variable retained were produced for 13,258 genes, and leave-one-out cross validation (LOOCV) was utilized (loss function: R cv.glmnet type.measure = “mse”) to select coefficients minimizing mean cross-validated error (regularization parameter: R predict s = “lambda.min”).

To examine allele-specific effects on transcription factor binding site affinity for the set of known PrCa variants, 25 base pair 3’ and 5’ flanking sequences were downloaded from the UCSC table browser [46] via Selenium webdriver automation. Next, FASTA sequences containing both the major and minor variant alleles were automatically analyzed through the sTRAP Transcription Factor Affinity Prediction webserver [47], with parameters “matrix file” = “transfac_2010.1 vertebrates”, “background model” = "human_promoters", and “Multiple test correction” = "Benjamini-Hochberg."

SUPPLEMENTARY REFERENCES

[1] Lindquist KJ, Paris PL, Hoffmann TJ, Cardin NJ, Kazma R, Mefford JA, et al. Mutational Landscape of Aggressive Prostate Tumors in African American Men. Cancer Res. 2016;76:1860-8.

[2] The Cancer Genome Atlas Research Network. The Molecular Taxonomy of Primary Prostate Cancer. Cell. 2015;163:1011-25.

[3] Kumar A, White TA, MacKenzie AP, Clegg N, Lee C, Dumpit RF, et al. Exome sequencing identifies a spectrum of mutation frequencies in advanced and lethal prostate cancers. Proc Natl Acad Sci U S A. 2011;108:17087-92.

[4] Cario CL, Witte JS. Samasy: an automated system for sample selection and robotic transfer. Biotechniques. 2018;65:357-60.

[5] Thermo Fisher Scientific Inc. Axiom Genotyping Solution Data Analysis Guide. 2017.

[6] McCarthy S, Das S, Kretzschmar W, Delaneau O, Wood AR, Teumer A, et al. A reference panel of 64,976 haplotypes for genotype imputation. Nat Genet. 2016;48:1279-83.

[7] 1000 Genomes Project Consortium, Auton A, Brooks LD, Durbin RM, Garrison EP, Kang HM, et al. A global reference for human genetic variation. Nature. 2015;526:68-74.

[8] https://github.com/szpiech/predictGMAP

[9] https://github.com/joepickrell/1000-genomes-genetic-maps/tree/master/interpolated_OMNI

[10] Szpiech ZA, Hernandez RD. selscan: an efficient multithreaded program to perform EHH-based scans for positive selection. Mol Biol Evol. 2014;31:2824-7.

[11] Akamatsu S, Takata R, Haiman CA, Takahashi A, Inoue T, Kubo M, et al. Common variants at 11q12, 10q26 and 3p11.2 are associated with prostate cancer susceptibility in Japanese. Nat Genet. 2012;44:426-9, S1.

[12] Al Olama AA, Kote-Jarai Z, Giles GG, Guy M, Morrison J, Severi G, et al. Multiple loci on 8q24 associated with prostate cancer susceptibility. Nat Genet. 2009;41:1058-60.

[13] Amin Al Olama A, Kote-Jarai Z, Schumacher FR, Wiklund F, Berndt SI, Benlloch S, et al. A meta-

analysis of genome-wide association studies to identify prostate cancer susceptibility loci associated with aggressive and non-aggressive disease. Hum Mol Genet. 2013;22:408-15.

[14] Cheng I, Chen GK, Nakagawa H, He J, Wan P, Laurie CC, et al. Evaluating genetic risk for prostate cancer among Japanese and Latinos. Cancer Epidemiol Biomarkers Prev. 2012;21:2048-58.

[15] Eeles RA, Kote-Jarai Z, Al Olama AA, Giles GG, Guy M, Severi G, et al. Identification of seven new prostate cancer susceptibility loci through a genome-wide association study. Nat Genet. 2009;41:1116-21.

[16] Eeles RA, Olama AA, Benlloch S, Saunders EJ, Leongamornlert DA, Tymrakiewicz M, et al. Identification of 23 new prostate cancer susceptibility loci using the iCOGS custom genotyping array. Nat Genet. 2013;45:385-91, 91e1-2.

[17] Gudmundsson J, Sulem P, Gudbjartsson DF, Blondal T, Gylfason A, Agnarsson BA, et al. Genome-wide association and replication studies identify four variants associated with prostate cancer susceptibility. Nat Genet. 2009;41:1122-6.

[18] Gudmundsson J, Sulem P, Manolescu A, Amundadottir LT, Gudbjartsson D, Helgason A, et al. Genome-wide association study identifies a second prostate cancer susceptibility variant at 8q24. Nat Genet. 2007;39:631-7.

[19] Gudmundsson J, Sulem P, Rafnar T, Bergthorsson JT, Manolescu A, Gudbjartsson D, et al. Common sequence variants on 2p15 and Xp11.22 confer susceptibility to prostate cancer. Nat Genet. 2008;40:281-3.

[20] Haiman CA, Chen GK, Blot WJ, Strom SS, Berndt SI, Kittles RA, et al. Genome-wide association study of prostate cancer in men of African ancestry identifies a susceptibility locus at 17q21. Nat Genet. 2011;43:570-3.

[21] Haiman CA, Patterson N, Freedman ML, Myers SR, Pike MC, Waliszewska A, et al. Multiple regions within 8q24 independently affect risk for prostate cancer. Nat Genet. 2007;39:638-44.

[22] Han Y, Signorello LB, Strom SS, Kittles RA, Rybicki BA, Stanford JL, et al. Generalizability of

established prostate cancer risk variants in men of African ancestry. Int J Cancer. 2015;136:1210-7.

[23] Jia L, Landan G, Pomerantz M, Jaschek R, Herman P, Reich D, et al. Functional enhancers at the gene-poor 8q24 cancer-linked locus. PLoS Genet. 2009;5:e1000597.

[24] Khor CC, Do T, Jia H, Nakano M, George R, Abu-Amero K, et al. Genome-wide association study identifies five new susceptibility loci for primary angle closure glaucoma. Nat Genet. 2016;48:556-62.

[25] Kote-Jarai Z, Olama AA, Giles GG, Severi G, Schleutker J, Weischer M, et al. Seven prostate cancer susceptibility loci identified by a multi-stage genome-wide association study. Nat Genet. 2011;43:785-91.

[26] Lindstrom S, Schumacher F, Siddiq A, Travis RC, Campa D, Berndt SI, et al. Characterizing associations and SNP-environment interactions for GWAS-identified prostate cancer risk markers--results from BPC3. PLoS One. 2011;6:e17142.

[27] Lindstrom S, Schumacher FR, Campa D, Albanes D, Andriole G, Berndt SI, et al. Replication of five prostate cancer loci identified in an Asian population--results from the NCI Breast and Prostate Cancer Cohort Consortium (BPC3). Cancer Epidemiol Biomarkers Prev. 2012;21:212-6.

[28] Schumacher FR, Berndt SI, Siddiq A, Jacobs KB, Wang Z, Lindstrom S, et al. Genome-wide association study identifies new prostate cancer susceptibility loci. Hum Mol Genet. 2011;20:3867-75.

[29] Sun J, Zheng SL, Wiklund F, Isaacs SD, Li G, Wiley KE, et al. Sequence variants at 22q13 are associated with prostate cancer risk. Cancer Res. 2009;69:10-5.

[30] Thomas G, Jacobs KB, Yeager M, Kraft P, Wacholder S, Orr N, et al. Multiple loci identified in a genome-wide association study of prostate cancer. Nat Genet. 2008;40:310-5.

[31] Xu J, Mo Z, Ye D, Wang M, Liu F, Jin G, et al. Genome-wide association study in Chinese men identifies two new prostate cancer risk loci at 9q31.2 and 19q13.4. Nat Genet. 2012;44:1231-5.

[32] Yeager M, Orr N, Hayes RB, Jacobs KB, Kraft P, Wacholder S, et al. Genome-wide association study of prostate cancer identifies a second risk locus at 8q24. Nat Genet. 2007;39:645-9.

[33] Hoffmann TJ, Van Den Eeden SK, Sakoda LC, Jorgenson E, Habel LA, Graff RE, et al. A large

multiethnic genome-wide association study of prostate cancer identifies novel risk variants and substantial ethnic differences. Cancer Discov. 2015;5:878-91.

[34] Schumacher FR, Al Olama AA, Berndt SI, Benlloch S, Ahmed M, Saunders EJ, et al. Association analyses of more than 140,000 men identify 63 new prostate cancer susceptibility loci. Nat Genet. 2018;50:928-36.

[35] Berndt SI, Wang Z, Yeager M, Alavanja MC, Albanes D, Amundadottir L, et al. Two susceptibility loci identified for prostate cancer aggressiveness. Nat Commun. 2015;6:6889.

[36] Marzec J, Mao X, Li M, Wang M, Feng N, Gou X, et al. A genetic study and meta-analysis of the genetic predisposition of prostate cancer in a Chinese population. Oncotarget. 2016;7:21393-403.

[37] Fehringer G, Kraft P, Pharoah PD, Eeles RA, Chatterjee N, Schumacher FR, et al. Cross-Cancer Genome-Wide Analysis of Lung, Ovary, Breast, Prostate, and Colorectal Cancer Reveals Novel Pleiotropic Associations. Cancer Res. 2016;76:5103-14.

[38] Conti DV, Wang K, Sheng X, Bensen JT, Hazelett DJ, Cook MB, et al. Two Novel Susceptibility Loci for Prostate Cancer in Men of African Ancestry. J Natl Cancer Inst. 2017;109.

[39] Wang M, Takahashi A, Liu F, Ye D, Ding Q, Qin C, et al. Large-scale association analysis in Asians identifies new susceptibility loci for prostate cancer. Nat Commun. 2015;6:8469.

[40] Thibodeau SN, French AJ, McDonnell SK, Cheville J, Middha S, Tillmans L, et al. Identification of candidate genes for prostate cancer-risk SNPs utilizing a normal prostate tissue eQTL data set. Nat Commun. 2015;6:8653.

[41] Loh PR, Danecek P, Palamara PF, Fuchsberger C, Y AR, H KF, et al. Reference-based phasing using the Haplotype Reference Consortium panel. Nat Genet. 2016;48:1443-8.

[42] Browning BL, Browning SR. Genotype Imputation with Millions of Reference Samples. Am J Hum Genet. 2016;98:116-26.

[43] Cock PJ, Antao T, Chang JT, Chapman BA, Cox CJ, Dalke A, et al. Biopython: freely available Python tools for computational molecular biology and bioinformatics. Bioinformatics. 2009;25:1422-3.

[44] Gamazon ER, Wheeler HE, Shah KP, Mozaffari SV, Aquino-Michaels K, Carroll RJ, et al. A gene-based association method for mapping traits using reference transcriptome data. Nat Genet. 2015;47:1091-8.

[45] Friedman J, Hastie T, Tibshirani R. Regularization Paths for Generalized Linear Models via Coordinate Descent. J Stat Softw. 2010;33:1-22.

[46] Karolchik D, Hinrichs AS, Furey TS, Roskin KM, Sugnet CW, Haussler D, et al. The UCSC Table Browser data retrieval tool. Nucleic Acids Res. 2004;32:D493-6.

[47] Manke T, Roider HG, Vingron M. Statistical modeling of transcription factor binding affinities predicts regulatory interactions. PLoS Comput Biol. 2008;4:e1000039.

Supplementary Table 1. Description of the Study Cohort

Ethnic Group		**Kaiser Permanente**		**UK Biobank**	
		Cases	**Controls**	**Cases**	**Controls**
European Ancestry	N	6,196	5,453	7,917	188,352
	Age [SD]	68.1 [7.9]	71.5 [10.8]	64.1 [5.6]	57.1 [8.1]
	BMI [SD]	26.9 [4.2]	27.0 [4.4]	27.6 [4.0]	27.8 [4.6]

* Subjects restricted to unrelated individuals.

Supplementary Table 2. Custom Microarray Design Modules

Module Name	Number of Variants*	Module Description
Missense	67,846	Nonsynonymous coding mutations
Tag	57,607	Variants tagging targeted content in other modules
Bad (EUR)	33,646	GWAS markers that did not previously pass QC on Affy EUR Array [1]
Bad (AFR)	33,584	GWAS markers that did not previously pass QC on Affy AFR Array [2]
Fine Mapping	29,096	Variants selected from previously reported prostate cancer GWAS loci
LOF	24,783	Loss-of-function coding mutations
WES_TCGA	24,167	Rare variants from TCGA prostate cancer patient normal tissue exomes [3]
Witte_somatic	17,792	Rare variants in windows around genes from important cancer pathways
CandGene4	17,095	Rare variants in windows around cancer-related candidate genes (4th tier)
Exome319_tier2	16,366	Variants from the Affy Exome319 exome chip (2nd tier)
CandGene1	13,586	Rare variants in windows around cancer-related candidate genes (1st tier)
CandGene3	9,465	Rare variants in windows around cancer-related candidate genes (3rd tier)
A_A_Rare	9,394	Rare variants from African American prostate cancer patient normal exomes
HSS	9,081	Rare variants from ENCODE PrCa cell line DNAse I hypersensitive regions
HGMD	8,557	Rare variants from HGMD database gene regions
Cosmic	7,233	Rare variants from recurrently somatically mutated cancer genes
CandGene5	7,095	Rare variants in windows around cancer-related candidate genes (5th tier)
tier2 eQTL	6,918	Variants associated with gene expression levels
cancer	6,706	UK Biobank cancer variation module
Exome319_tier1	6,402	Variants from the Affy Exome319 exome chip (1st tier)
Neanderthal	5,680	Variants thought to be introduced during Human-Neanderthal introgression
LOF novel	5,194	Loss-of-function coding mutations
HGMD novelprescue	5,132	Rare variants from HGMD database gene regions
8k eQTL	4,662	Variants associated with gene expression levels in different tissues
GWAS compatibility	3,992	Variants for boosting GWAS coverage
CandGene2	2,597	Rare variants in windows around cancer-related candidate genes (2nd tier)
WES_dbgap	1,426	Rare variants from dbGaP prostate cancer patient normal tissue exomes [4]
HLA/KIR	1,408	Variants in HLA / KIR genes
ADME	1,183	Pharmacogenomics variants
chrY	806	Variants located on chromosome Y
ASHG	742	Variants from cancer genes presented at 2013 ASHG conference
AfAmrImputed	583	African American GWAS imputed variants
GWAS_enrichment_tier1.4	454	Variants from the NHGRI GWAS catalog (4th tier)
KIR	418	Variants in the KIR gene
BioBank1_LoF_tier1	367	Loss-of-function coding mutations
Kaiser GWAS	283	Variants associated in GWAS in the Kaiser Permanente RPGEH cohort
Diabetes_Metabochip	274	Variants related to metabolic, cardiovascular, and anthropometric traits
Telomere	261	Variants associated with leukocyte telomere length
GWAS_enrichment_tier1.1	243	Variants from the NHGRI GWAS catalog (1st tier)

Module Name	Number of Variants*	Module Description
Height	221	Variants associated with height
Diabetes_GWAS	211	Variants associated with diabetes
ApoE	203	Variants in the ApoE gene
BrCa	183	Variants associated with breast cancer risk
chrMT	180	Variants located on the mitochondrial chromosome
GWAS_enrichment_tier1.3	140	Variants from the NHGRI GWAS catalog (3rd tier)
Ovarian	137	Variants associated with ovarian cancer risk
Blood eQTL	125	Variants associated with gene expression levels in blood cells
GWAS_enrichment_tier1.2	51	Variants from the NHGRI GWAS catalog (2nd tier)
CandGene0	50	Rare variants in windows around cancer-related candidate genes (0th tier)
CandGene6	24	Rare variants in windows around cancer-related candidate genes (6th tier)
Radiogen	4	Variants associated with radiogenomic phenotypes
special	2	Variants to be forced on the array
Alzheimers	2	Variants associated with Alzheimer's risk
CandGene1	1	Variants from 1st list of cancer-related candidate genes

* Total sums to greater than the number of genotyped probesets because certain probesets were members of multiple modules.

Supplementary Table 3. Information and Summary Statistics for 187 Variants Modeled in Prostate Cancer Polygenic Risk Score

dbSNP rsid	Cytogenetic Band	hg19 Position	Risk Allele	Ref Allele	Odds Ratio	Source of Summary Statistics
rs636291	1p35	10556097	A	G	1.18	Hoffmann et al. 2015
rs56391074	1p22.3	88210715	A	AT	1.05	Schumacher et al. 2018
rs17599629	1q21	150658287	G	A	1.08	Hoffmann et al. 2015
rs34579442	1q21.3	153899900	C	CT	1.07	Schumacher et al. 2018
rs1218582	1q21	154834183	G	A	1.06	Hoffmann et al. 2015
rs4245739	1q32	204518842	A	C	1.1	Hoffmann et al. 2015
rs1775148	1q32	205757824	C	T	1.06	Hoffmann et al. 2015
rs62106670	2p25.1	8597123	T	C	1.05	Schumacher et al. 2018
rs11902236	2p25	10117868	A	G	1.07	Hoffmann et al. 2015
rs9287719	2p25	10710730	C	T	1.06	Hoffmann et al. 2015
rs13385191	2p24	20888265	G	A	1.07	Hoffmann et al. 2015
rs1465618	2p21	43553949	A	G	1.08	Hoffmann et al. 2015
rs721048	2p15	63131731	A	G	1.15	Hoffmann et al. 2015
rs2430386	2p15	63178111	T	C	1.14	Berndt et al. 2015
rs74702681	2p14	66652885	T	C	1.17	Schumacher et al. 2018
rs10187424	2p11	85794297	A	G	1.09	Hoffmann et al. 2015
rs11691517	2q13	111893096	T	G	1.07	Schumacher et al. 2018
rs13016083	2q22.3	148570945	T	C	1.13	Hoffmann et al. 2015
rs12621278	2q31	173311553	A	G	1.33	Hoffmann et al. 2015
rs34925593	2q31.1	174234547	C	T	1.05	Schumacher et al. 2018
rs59308963	2q33.1	202123479	T	TATTCTGTC	1.05	Schumacher et al. 2018
rs2292884	2q37	238443226	G	A	1.14	Hoffmann et al. 2015
rs3771570	2q37	242382864	A	G	1.12	Hoffmann et al. 2015
rs2660753	3p12	87110674	T	C	1.13	Hoffmann et al. 2015
rs7629490	3p11	87241497	T	C	1.15	Schumacher et al. 2011
rs2055109	3p11	87467332	C	T	1.2	Hoffmann et al. 2015
rs1283104	3q13.12	106962521	G	C	1.05	Schumacher et al. 2018
rs7611694	3q13	113275624	A	C	1.1	Hoffmann et al. 2015
rs10934853	3q21	128038373	A	C	1.12	Hoffmann et al. 2015
rs6763931	3q23	141102833	T	C	1.04	Hoffmann et al. 2015
rs182314334	3q25.1	152004202	T	C	1.09	Schumacher et al. 2018
rs142436749	3q26.2	169093100	G	A	1.25	Schumacher et al. 2018
rs71277158	3q26.2	169999216	T	G	1.22	Berndt et al. 2015
rs10936632	3q26	170130102	A	C	1.11	Hoffmann et al. 2015
rs10009409	4q13	73855253	T	C	1.08	Hoffmann et al. 2015
rs1894292	4q13	74349158	G	A	1.1	Hoffmann et al. 2015
rs12500426	4q22	95514609	A	C	1.08	Hoffmann et al. 2015
rs17021918	4q22	95562877	C	T	1.11	Hoffmann et al. 2015
rs7679673	4q24	106061534	C	A	1.1	Hoffmann et al. 2015
rs6825684	4q24	106084643	G	A	1.17	Fehringer et al. 2016
rs2242652	5p15	1280028	G	A	1.15	Hoffmann et al. 2015
rs12653946	5p15	1895829	T	C	1.1	Hoffmann et al. 2015
rs2121875	5p12	44365545	G	T	1.05	Hoffmann et al. 2015
rs10793821	5q31.1	133836209	T	C	1.05	Schumacher et al. 2018
rs76551843	5q35.1	169172133	A	G	1.31	Schumacher et al. 2018

dbSNP rsid	Cytogenetic Band	hg19 Position	Risk Allele	Ref Allele	Odds Ratio	Source of Summary Statistics
rs6869841	5q35	172939426	A	G	1.07	Hoffmann et al. 2015
rs4976790	5q35.3	177968915	T	G	1.08	Schumacher et al. 2018
rs4713266	6p24	11219030	C	T	1.06	Hoffmann et al. 2015
rs7767188	6p22	30073776	A	G	1.07	Hoffmann et al. 2015
rs12665339	6p21.33	30601232	G	A	1.06	Schumacher et al. 2018
rs130067	6p21	31118511	G	T	1.05	Hoffmann et al. 2015
rs3096702	6p21	32192331	A	G	1.07	Hoffmann et al. 2015
rs115306967	6p21	32400939	G	C	1.06	Hoffmann et al. 2015
rs9296068	6p21.32	32988695	T	G	1.05	Schumacher et al. 2018
rs9469899	6p21.31	34793124	A	G	1.05	Schumacher et al. 2018
rs1983891	6p21	41536427	T	C	1.09	Hoffmann et al. 2015
rs4711748	6p21.1	43694598	T	C	1.05	Schumacher et al. 2018
rs9443189	6q14	76495882	G	A	1.08	Hoffmann et al. 2015
rs2273669	6q21	109285189	G	A	1.07	Hoffmann et al. 2015
rs339331	6q22	117210052	T	C	1.08	Hoffmann et al. 2015
rs1933488	6q25	153441079	A	G	1.12	Hoffmann et al. 2015
rs651164	6q25.3	160581374	G	A	1.14	Marzec et al. 2016
rs4646284	6q25.3	160581544	TG	T	1.18	Hoffmann et al. 2015
rs9364554	6q25	160833664	T	C	1.08	Hoffmann et al. 2015
rs138004030	6q27	170475879	G	A	1.27	Schumacher et al. 2018
rs527510716	7p22.3	1944537	C	G	1.06	Schumacher et al. 2018
rs11452686	7p21.1	20414110	T	TA	1.05	Schumacher et al. 2018
rs12155172	7p15	20994491	A	G	1.11	Hoffmann et al. 2015
rs10486567	7p15	27976563	G	A	1.19	Hoffmann et al. 2015
rs17621345	7p14.1	40875192	A	C	1.07	Schumacher et al. 2018
rs56232506	7p12	47437244	A	G	1.06	Hoffmann et al. 2015
rs6465657	7q21	97816327	C	T	1.11	Hoffmann et al. 2015
rs2928679	8p21	23438975	T	C	1.05	Hoffmann et al. 2015
rs1512268	8p21	23526463	A	G	1.18	Hoffmann et al. 2015
rs11135910	8p21	25892142	A	G	1.11	Hoffmann et al. 2015
rs12543663	8q24	127924659	C	A	1.08	Hoffmann et al. 2015
rs1487232	8q24.21	128005247	A	G	1.33	Schumacher et al. 2011
rs10086908	8q24	128011937	T	C	1.15	Hoffmann et al. 2015
rs1016343	8q24	128093297	T	C	1.25	Hoffmann et al. 2015
rs13252298	8q24	128095156	A	G	1.19	Hoffmann et al. 2015
rs6983561	8q24	128106880	C	A	1.47	Hoffmann et al. 2015
rs116041037	8q24	128131809	A	G	2.45	Hoffmann et al. 2015
rs16902094	8q24.21	128320346	G	A	1.21	Marzec et al. 2016
rs445114	8q24	128323181	T	C	1.14	Hoffmann et al. 2015
rs16902104	8q24	128340908	T	C	1.21	Hoffmann et al. 2015
rs6983267	8q24	128413305	G	T	1.23	Hoffmann et al. 2015
rs6999921	8q24	128440928	G	A	1.23	Schumacher et al. 2011
rs7000448	8q24	128441170	T	C	1.14	Hoffmann et al. 2015
rs1447293	8q24	128472320	C	T	1.14	Schumacher et al. 2011
rs11986220	8q24	128531689	A	T	1.36	Hoffmann et al. 2015
rs12549761	8q24	128540776	C	G	1.38	Conti et al. 2017
rs1048169	9p22.1	19055965	C	T	1.06	Schumacher et al. 2018
rs17694493	9p21	22041998	G	C	1.08	Hoffmann et al. 2015

dbSNP rsid	Cytogenetic Band	hg19 Position	Risk Allele	Ref Allele	Odds Ratio	Source of Summary Statistics
rs10122495	9p13.3	34049779	T	A	1.05	Schumacher et al. 2018
rs817826	9q31	110156300	C	T	1.41	Hoffmann et al. 2015
rs1571801	9q33	124427373	A	C	1.07	Hoffmann et al. 2015
rs1182	9q34.11	132576060	A	C	1.06	Schumacher et al. 2018
rs141536087	10p15.3	854691	GCGCA	G	1.08	Schumacher et al. 2018
rs76934034	10q11	46082985	T	C	1.13	Hoffmann et al. 2015
rs10993994	10q11	51549496	T	C	1.23	Hoffmann et al. 2015
rs1935581	10q23.31	90195149	C	T	1.05	Schumacher et al. 2018
rs3850699	10q24	104414221	A	G	1.1	Hoffmann et al. 2015
rs7094871	10q25.2	114712154	G	C	1.04	Schumacher et al. 2018
rs2252004	10q26	122844709	G	T	1.16	Hoffmann et al. 2015
rs4962416	10q26	126696872	C	T	1.09	Hoffmann et al. 2015
rs1881502	11p15.5	1507512	T	C	1.06	Schumacher et al. 2018
rs7127900	11p15	2233574	A	G	1.22	Hoffmann et al. 2015
rs61890184	11p15.4	7547587	A	G	1.07	Schumacher et al. 2018
rs547171081	11p11.2	47421962	CGG	C	1.05	Schumacher et al. 2018
rs1938781	11q12	58915110	C	T	1.16	Hoffmann et al. 2015
rs2277283	11q12.3	61908440	C	T	1.06	Schumacher et al. 2018
rs12785905	11q13.2	66951965	C	G	1.12	Schumacher et al. 2018
rs12418451	11q13	68935419	A	G	1.14	Marzec et al. 2016
rs11228565	11q13	68978580	A	G	1.23	Marzec et al. 2016
rs10896449	11q13	68994667	G	A	1.19	Hoffmann et al. 2015
rs11228594	11q13	69023087	A	G	1.15	Schumacher et al. 2011
rs7940107	11q13	69027770	A	G	1.2	Schumacher et al. 2011
rs11290954	11q13.5	76260543	AC	A	1.06	Schumacher et al. 2018
rs11568818	11q22	102401661	A	G	1.1	Hoffmann et al. 2015
rs1800057	11q22.3	108143456	G	C	1.16	Schumacher et al. 2018
rs11214775	11q23	113807181	G	A	1.07	Hoffmann et al. 2015
rs138466039	11q24.2	125054793	T	C	1.32	Schumacher et al. 2018
rs878987	11q25	134266372	G	A	1.07	Schumacher et al. 2018
rs2066827	12p13.1	12871099	T	G	1.06	Schumacher et al. 2018
rs10845938	12p13.1	14416918	G	A	1.06	Schumacher et al. 2018
rs80130819	12q13	48419618	A	C	1.14	Hoffmann et al. 2015
rs10875943	12q13	49676010	C	T	1.07	Hoffmann et al. 2015
rs902774	12q13	53273904	A	G	1.17	Hoffmann et al. 2015
rs7968403	12q14.2	65012824	T	C	1.06	Schumacher et al. 2018
rs5799921	12q21.33	90160530	GA	G	1.06	Schumacher et al. 2018
rs1270884	12q24	114685571	A	G	1.07	Hoffmann et al. 2015
rs7295014	12q24.33	133067989	G	A	1.05	Schumacher et al. 2018
rs9600079	13q22	73728139	T	G	1.01	Hoffmann et al. 2015
rs1004030	14q11.2	23305649	T	C	1.05	Schumacher et al. 2018
rs11629412	14q13.3	37138294	C	G	1.06	Schumacher et al. 2018
rs8008270	14q22	53372330	G	A	1.12	Hoffmann et al. 2015
rs7153648	14q23	61122526	C	G	1.11	Hoffmann et al. 2015
rs34582366	14q23.1	61933357	G	T	1.42	Hoffmann et al. 2015
rs7141529	14q24	69126744	G	A	1.09	Hoffmann et al. 2015
rs8014671	14q24	71092256	G	A	1.06	Hoffmann et al. 2015
rs4924487	15q15.1	40922915	C	G	1.06	Schumacher et al. 2018

dbSNP rsid	Cytogenetic Band	hg19 Position	Risk Allele	Ref Allele	Odds Ratio	Source of Summary Statistics
rs6493618	15q21	53537453	T	C	2	Wang et al. 2015
rs33984059	15q21.3	56385868	A	G	1.19	Schumacher et al. 2018
rs112293876	15q22.31	66764641	C	CA	1.06	Schumacher et al. 2018
rs11863709	16q21	57654576	C	T	1.16	Schumacher et al. 2018
rs12051443	16q22	71691329	A	G	1.06	Hoffmann et al. 2015
rs201158093	16q23.3	82178893	TAA	TA	1.05	Schumacher et al. 2018
rs684232	17p13	618965	G	A	1.1	Hoffmann et al. 2015
rs28441558	17p13.1	7803118	C	T	1.16	Schumacher et al. 2018
rs142444269	17q11.2	30098749	C	T	1.07	Schumacher et al. 2018
rs11649743	17q12	36074979	G	A	1.15	Hoffmann et al. 2015
rs7501939	17q12	36101156	C	T	1.22	Hoffmann et al. 2015
rs11650494	17q21	47345186	A	G	1.15	Hoffmann et al. 2015
rs7210100	17q21	47436749	A	G	1.51	Hoffmann et al. 2015
rs2680708	17q22	56456120	G	A	1.05	Schumacher et al. 2018
rs1859962	17q24	69108753	G	T	1.19	Hoffmann et al. 2015
rs8093601	18q21.2	51772473	C	G	1.05	Schumacher et al. 2018
rs28607662	18q21.2	53230859	C	T	1.08	Schumacher et al. 2018
rs12956892	18q21.32	56746315	T	G	1.05	Schumacher et al. 2018
rs533722308	18q21.33	60961193	CT	C	1.05	Schumacher et al. 2018
rs10460109	18q22.3	73036165	T	C	1.05	Schumacher et al. 2018
rs7241993	18q23	76773973	G	A	1.09	Hoffmann et al. 2015
rs11666569	19p13.11	17214073	C	T	1.05	Schumacher et al. 2018
rs118005503	19q12	32167803	G	C	1.09	Schumacher et al. 2018
rs8102476	19q13	38735613	C	T	1.12	Hoffmann et al. 2015
rs11672691	19q13	41985587	G	A	1.08	Hoffmann et al. 2015
rs61088131	19q13.2	42700947	T	C	1.06	Schumacher et al. 2018
rs2735839	19q13	51364623	G	A	1.15	Hoffmann et al. 2015
rs103294	19q13	54797848	C	T	1.28	Hoffmann et al. 2015
rs11480453	20q11.21	31347512	C	CA	1.05	Schumacher et al. 2018
rs12480328	20q13	49527922	T	C	1.13	Hoffmann et al. 2015
rs6091758	20q13.2	52455205	G	A	1.07	Schumacher et al. 2018
rs2427345	20q13	61015611	G	A	1.06	Hoffmann et al. 2015
rs6062509	20q13	62362563	A	C	1.12	Hoffmann et al. 2015
rs1041449	21q22	42901421	G	A	1.06	Hoffmann et al. 2015
rs2238776	22q11	19757892	G	A	1.08	Hoffmann et al. 2015
rs9625483	22q12.1	28888939	A	G	1.14	Schumacher et al. 2018
rs9623117	22q13	40452119	C	T	1.18	Hoffmann et al. 2015
rs5759167	22q13	43500212	G	T	1.16	Hoffmann et al. 2015
rs742134	22q13	43518275	G	A	1.2	Schumacher et al. 2011
rs2405942	23p22	9814135	A	G	1.14	Hoffmann et al. 2015
rs17321482	23p22.2	11482634	C	T	1.07	Schumacher et al. 2018
rs5945572	23p11	51229683	A	G	1.23	Hoffmann et al. 2015
rs2807031	23p11	52896949	C	T	1.07	Hoffmann et al. 2015
rs5919432	23q12	67021550	A	G	1.06	Hoffmann et al. 2015
rs6625711	23q13	70139850	A	T	1.04	Hoffmann et al. 2015
rs4844289	23q13	70407983	G	A	1.04	Hoffmann et al. 2015

Supplementary Table 4. Polygenic Risk Score Performance

Cohort and Ethnic Group	**Polygenic Risk Score Decile**	**Odds Ratio**	**Lower 95% CI**	**Upper 95% CI**	***P*-Value**
KP + UKB European Ancestry	1	--	--	--	--
	2	1.55	1.37	1.77	1.54E-11
	3	2.07	1.82	2.35	5.53E-30
	4	2.37	2.09	2.68	2.08E-42
	5	2.62	2.31	2.96	6.78E-53
	6	3.06	2.71	3.46	3.44E-72
	7	3.70	3.27	4.18	2.59E-98
	8	4.24	3.76	4.79	3.97E-121
	9	4.76	4.22	5.37	2.62E-143
	10	7.83	6.94	8.84	1.83E-245
KP European Ancestry	1	--	--	--	--
	2	1.50	1.26	1.79	5.87E-06
	3	2.02	1.70	2.40	1.79E-15
	4	2.46	2.07	2.93	1.51E-24
	5	2.53	2.13	3.01	5.99E-26
	6	2.83	2.38	3.37	3.32E-32
	7	3.38	2.84	4.02	3.45E-43
	8	3.95	3.32	4.71	1.38E-53
	9	4.09	3.43	4.87	4.10E-56
	10	7.10	5.90	8.54	1.82E-96
UKB European Ancestry	1	--	--	--	--
	2	1.61	1.31	1.98	4.41E-06
	3	2.12	1.74	2.59	7.18E-14
	4	2.29	1.89	2.78	4.85E-17
	5	2.79	2.30	3.38	1.36E-25
	6	3.25	2.69	3.93	4.20E-34
	7	4.04	3.34	4.89	1.32E-47
	8	4.37	3.62	5.26	2.84E-54
	9	5.24	4.36	6.30	6.29E-70
	10	8.48	7.07	10.2	1.74E-117

Supplementary Figure 1a. Custom Microarray Marker Content

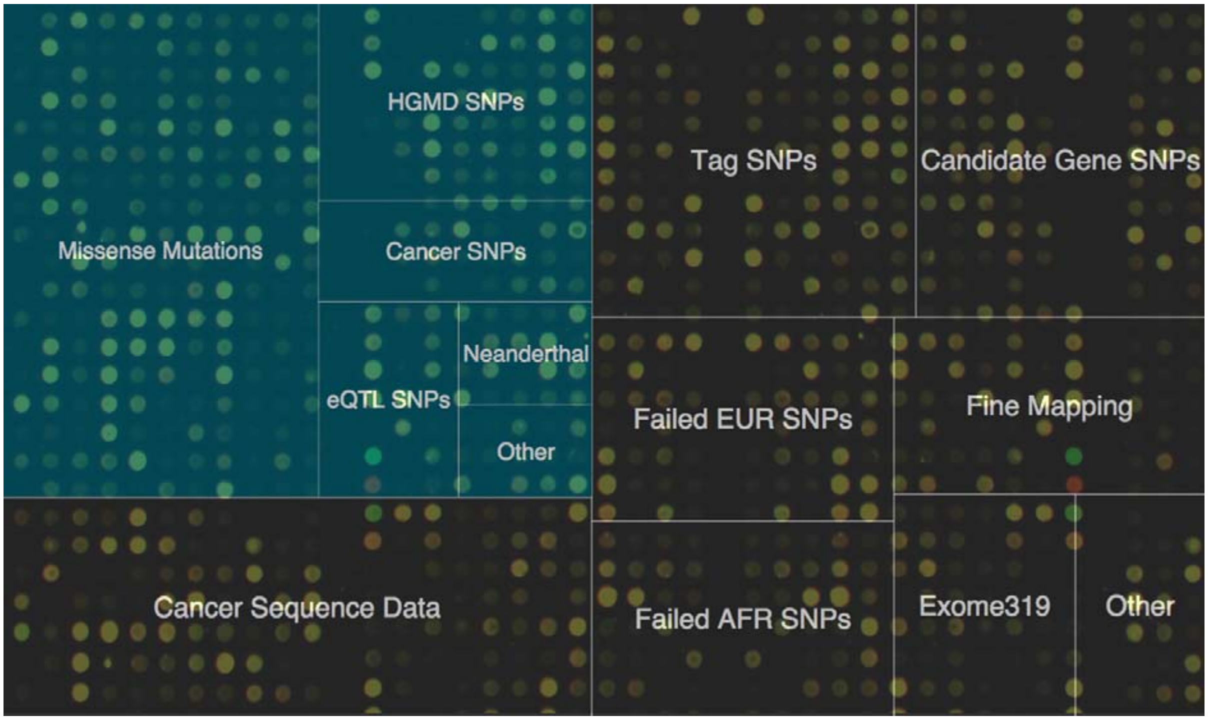

Supplementary Figure 1b. SNP Selection Algorithm

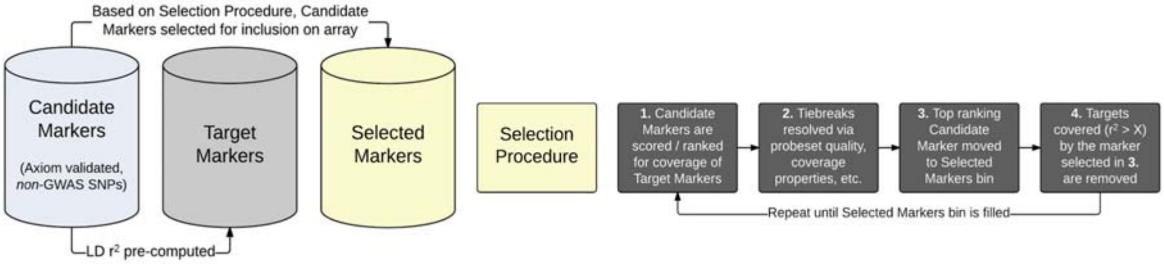
Based on Selection Procedure, Candidate Markers selected for inclusion on array
Candidate Markers
(Axiom validated, non-GWAS SNPs)
Target Markers
Selected Markers
LD r² pre-computed
Selection Procedure
1. Candidate Markers are scored / ranked for coverage of Target Markers
2. Tiebreaks resolved via probeset quality, coverage properties, etc.
3. Top ranking Candidate Marker moved to Selected Markers bin
4. Targets covered (r² > X) by the marker selected in 3. are removed
Repeat until Selected Markers bin is filled

Supplementary Figure 1 Legend. Custom Array Design. S1a. The relative fractions of Selected Markers are grouped by their source and illustrated to scale (total of 416,047 probesets). Teal colored cells derive from the UK Biobank Array modules and include a diverse set of curated and functionally relevant mutations. S1b. SNP Selection was conducted according to a greedy algorithm. In a single iteration of the algorithm, Candidate Markers are ranked for coverage of Target Markers, the best candidate is moved to the set of Selected Markers, and the candidates are re-ranked. The algorithm allows for markers to be "pre-selected" by placement in the Selected Markers set upon initialization, and runs until the Selected Markers bin equals a certain maximum value. Probesets for the resulting selected markers are included in the fabrication of the custom microarray chip.

Supplementary Figure 2a. Sample Quality Control

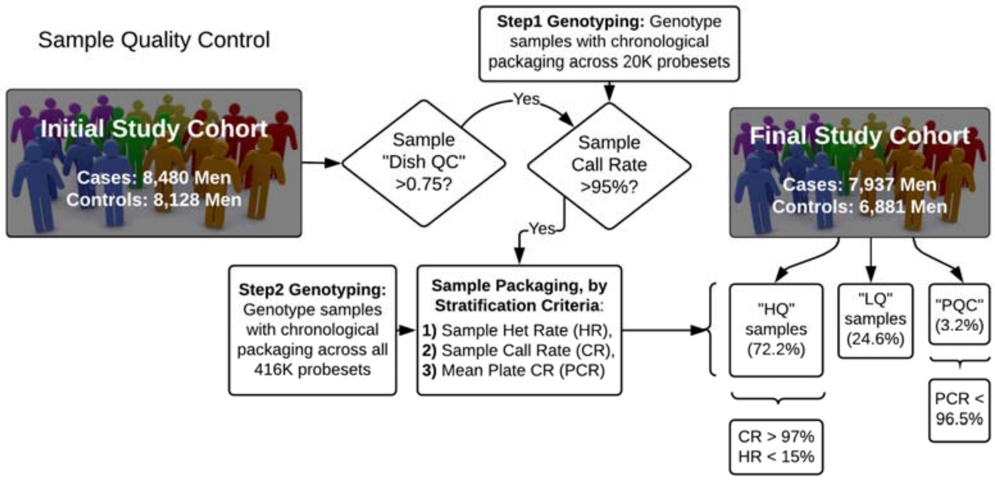
Sample Quality Control
Step1 Genotyping: Genotype samples with chronological packaging across 20K probesets
Initial Study Cohort
Cases: 8,480 Men
Controls: 8,128 Men
Sample "Dish QC" >0.75?
Yes
Sample Call Rate >95%?
Yes
Final Study Cohort
Cases: 7,937 Men
Controls: 6,881 Men
Step2 Genotyping: Genotype samples with chronological packaging across all 416K probesets
Sample Packaging, by Stratification Criteria: 1) Sample Het Rate (HR), 2) Sample Call Rate (CR), 3) Mean Plate CR (PCR)
"HQ" samples (72.2%)
"LQ" samples (24.6%)
"PQC" (3.2%)
CR > 97%
HR < 15%
PCR < 96.5%

Supplementary Figure 2b. Variant Quality Control

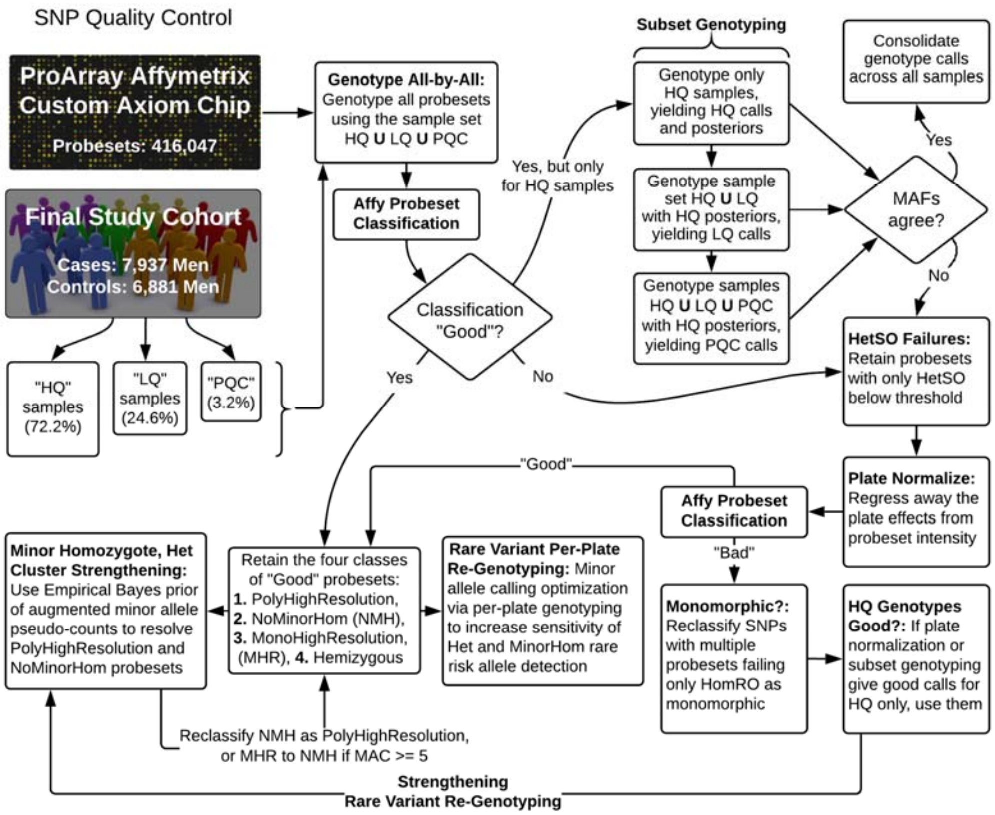
SNP Quality Control
ProArray Affymetrix Custom Axiom Chip
Probesets: 416,047
Final Study Cohort
Cases: 7,937 Men
Controls: 6,881 Men
"HQ" samples (72.2%)
"LQ" samples (24.6%)
"PQC" (3.2%)
Genotype All-by-All: Genotype all probesets using the sample set HQ U LQ U PQC
Affy Probeset Classification
Classification "Good"?
Yes
No
Yes, but only for HQ samples
Subset Genotyping
Genotype only HQ samples, yielding HQ calls and posteriors
Genotype sample set HQ U LQ with HQ posteriors, yielding LQ calls
Genotype samples HQ U LQ U PQC with HQ posteriors, yielding PQC calls
Consolidate genotype calls across all samples
Yes
MAFs agree?
No
HetSO Failures: Retain probesets with only HetSO below threshold
Plate Normalize: Regress away the plate effects from probeset intensity
Affy Probeset Classification
"Good"
"Bad"
Monomorphic?: Reclassify SNPs with multiple probesets failing only HomRO as monomorphic
HQ Genotypes Good?: If plate normalization or subset genotyping give good calls for HQ only, use them
Rare Variant Per-Plate Re-Genotyping: Minor allele calling optimization via per-plate genotyping to increase sensitivity of Het and MinorHom rare risk allele detection
Retain the four classes of "Good" probesets: 1. PolyHighResolution, 2. NoMinorHom (NMH), 3. MonoHighResolution, (MHR), 4. Hemizygous
Minor Homozygote, Het Cluster Strengthening: Use Empirical Bayes prior of augmented minor allele pseudo-counts to resolve PolyHighResolution and NoMinorHom probesets
Reclassify NMH as PolyHighResolution, or MHR to NMH if MAC >= 5
Strengthening
Rare Variant Re-Genotyping

Supplementary Figure 2 Legend. Sample and Variant Quality Control Workflows. 2a. Sample Quality Control. 2b. Variant Quality Control.

Supplementary Figure 3. Genotype Imputation Workflow

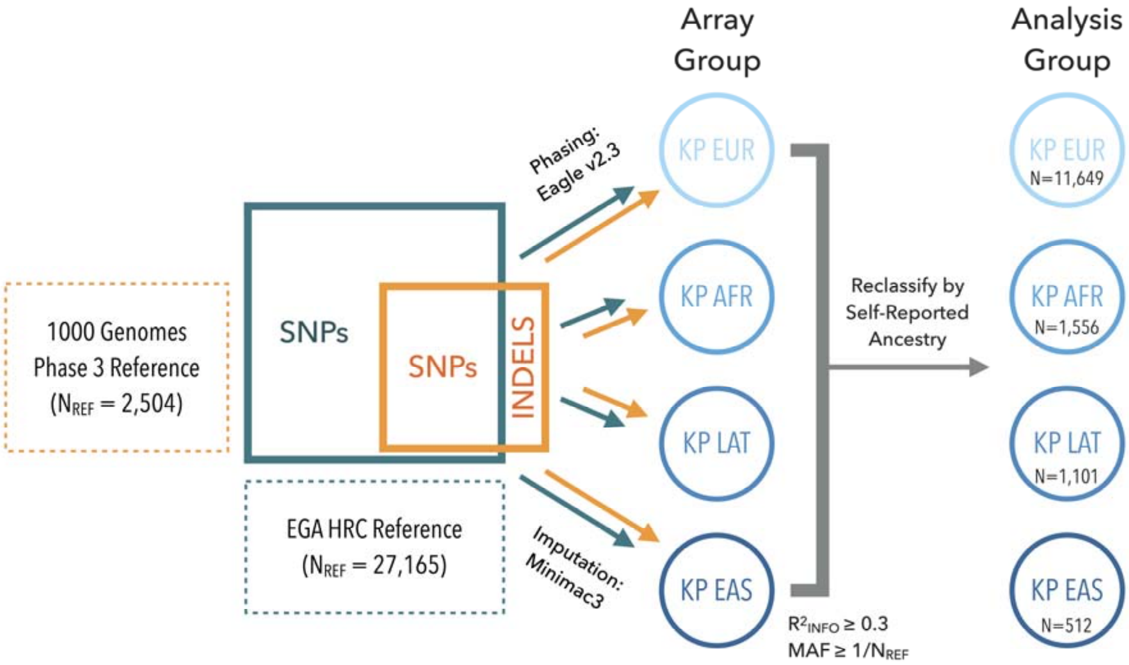

Supplementary Figure 3 Legend. Genotype Imputation Workflow. Depicted is the procedure implemented for imputing the Kaiser Permanente (KP) genotype data, from four ethnic groups: European ancestry (EUR), African ancestry (AFR), Latino ancestry (LAT), and East Asian ancestry (EAS). KP data were phased, reference-free (cohort-based), into haplotype-resolved genomes using Eagle v2.3. Next, single nucleotide polymorphisms (SNPs) were imputed using Minimac3 and a combined reference panel of Haplotype Reference Consortium (number of references, N_{REF}: 27,165) and 1000 Genomes Project Phase III (number of references: 2,504) reference genomes. Furthermore, indel variants were imputed using the 1000 Genomes Project Phase III reference. Imputed SNPs and indels were combined, filtered based on imputation r^2 (R^2_{INFO}) and minor allele frequency (MAF), and resegregated into analysis groups based on their self-reported ancestry (as opposed to the array groups with which they were genotyped).

Supplementary Figure 4. SKAT Gene-Based Rare Variant (MAF < 1%) Meta-Analysis of KP and UKB European-Ancestry Subjects

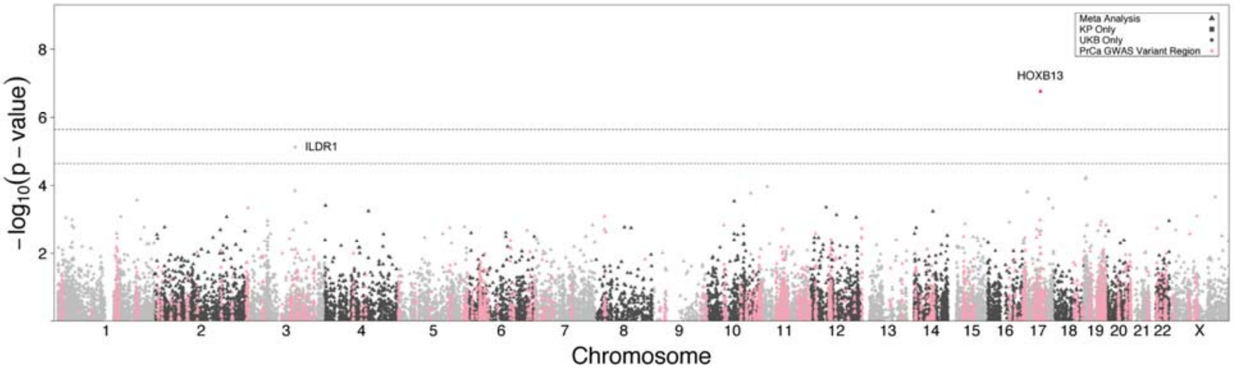

Supplementary Figure 4 Legend. Gene-Based Test Manhattan Plot. Manhattan plot of associations for a gene-based meta-analysis between the Kaiser Permanente and UK Biobank. The associations (-$\log_{10}$(*P*-value), Y-axis) are plotted against the chromosome (1-22, X) and position (X-axis) of the modeled genes, with thresholds for Bonferroni-significant ($P < 2.5*10^{-6}$) and suggestive ($2.5*10^{-5} < P < 2.5*10^{-6}$) associations illustrated by dashed grey lines. Non-significant genes on odd and even chromosomes are colored in alternating shades. Triangular data points illustrate variants that were meta-analyzed between KP and UKB, while squares and circles indicate genes present exclusively in the KP or UKB summary statistics, respectively. Previously discovered PrCa loci are highlighted in pink for a 2 Mb window around the reported lead variant.

Supplementary Figure 5a. 17q12 Locus Manhattan Plot

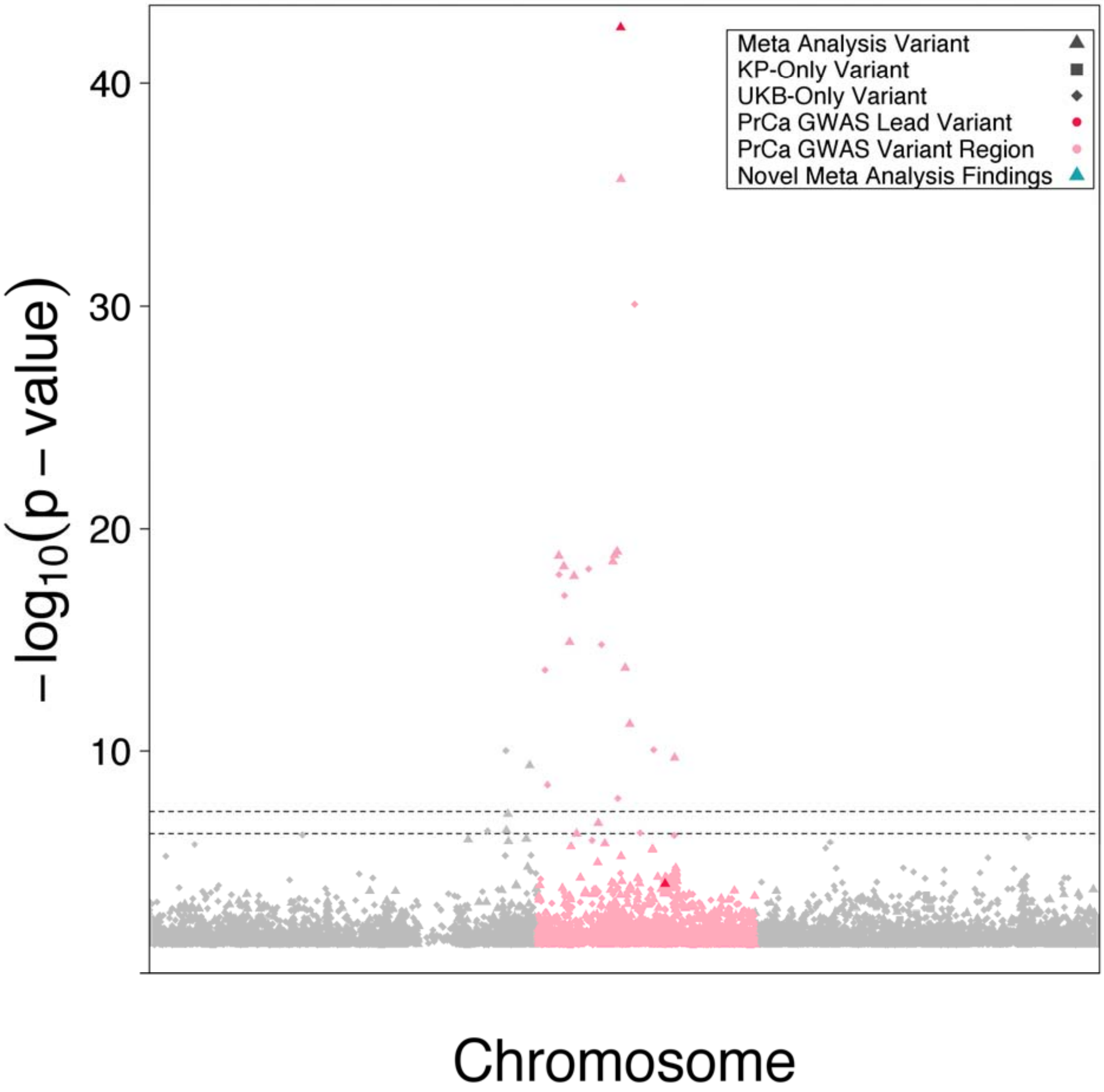

Supplementary Figure 5b. Linkage Disequilibrium at rare HOXB13 G84E missense variant rs138213197 (17q12)

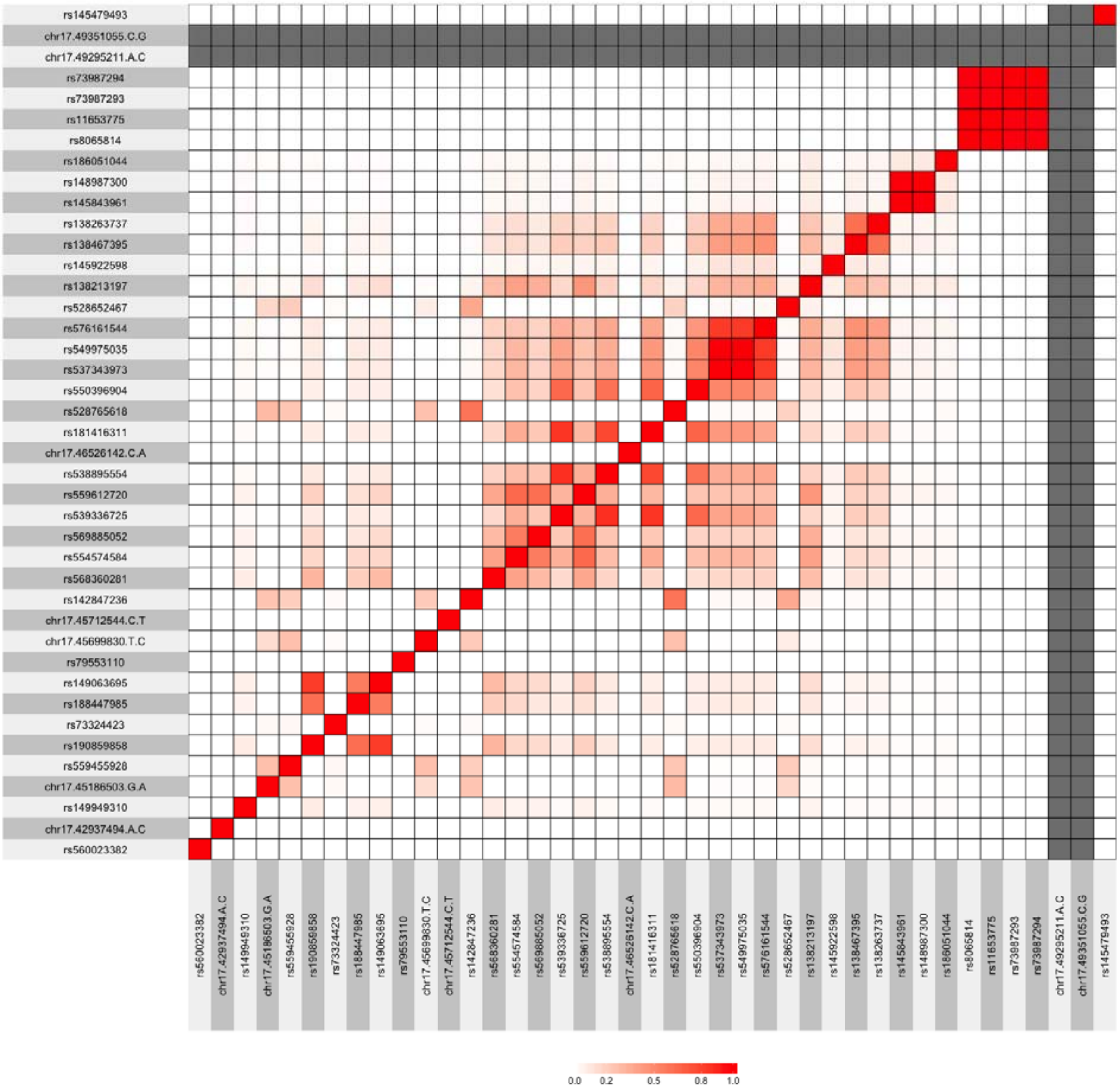

Supplementary Figure 5 Legend. Associations and Linkage Disequilibrium at 17q12. S5a. Manhattan plot for meta-analysis of Kaiser Permanente and UK Biobank genotypes at the 17q12 locus, centered around the HOXB13 G84E missense variant rs138213197. Variants within 1Mb of the highly significant association at the rs138213197 SNP ($P < 1*10^{-40}$) are colored in pink, demonstrating the width of the association peak. S5b. Linkage disequilibrium (LD) heatmap plot for all 17q12 variants with $P < 5*10^{-6}$. Long range LD (beyond 1Mb) with respect to rs138213197 is illustrated.

Supplementary Figure 6. Polygenic Risk Score Modeling of Prostate Cancer Across KP and UKB Subjects

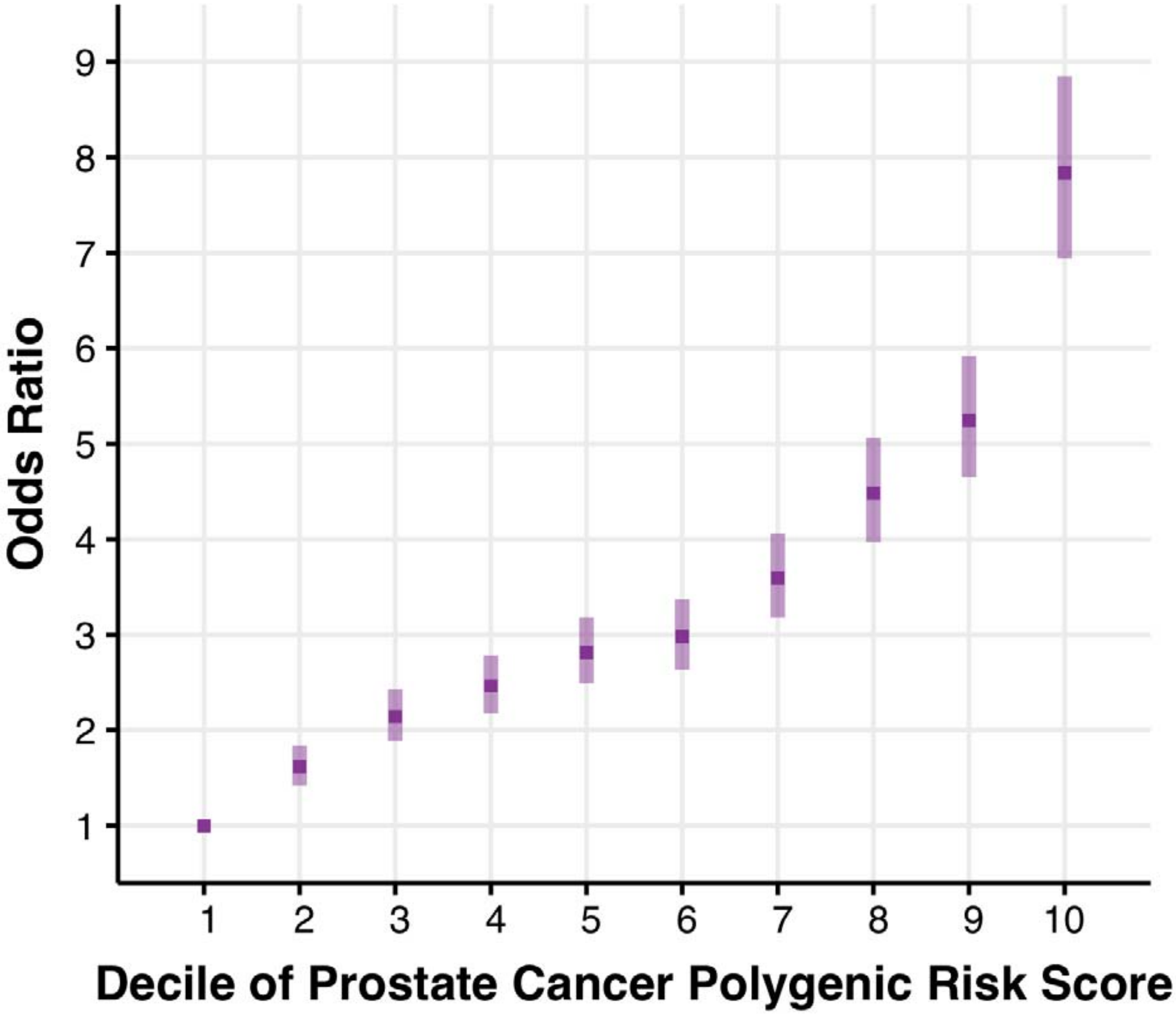

Supplementary Figure 6 Legend: “Prostate Cancer Polygenic Risk Score Performance. A polygenic risk score (PRS) of 187 previously reported prostate cancer (PrCa) risk variants was applied to subjects of European ancestry from two cohorts (Kaiser Permanente and UK Biobank). The Y-axis illustrates the magnitude of the odds ratio and 95% confidence interval for the association between PRS values and PrCa case-control status within a given decile of the PRS, in relation to the bottom decile as a reference group. Models were adjusted for age, body mass index, and principal components of ancestry.”